Journal Pre-proof


# Pulse waveform and current direction alter network-level TMS-induced functional connectivity: Evidence from TMS-EEG

Delia Lucarelli , Giacomo Guidali , Roberto Guidotti , Giulia Pieramico , Nadia Bolognini , Gian Luca Romani , Vittorio Pizzella , Laura Marzetti

PII: S1053-8119(26)00112-6
DOI: https://doi.org/10.1016/j.neuroimage.2026.121794
Reference: YNIMG 121794

To appear in: *NeuroImage*

Received date: 10 June 2025
Revised date: 16 January 2026
Accepted date: 6 February 2026

Please cite this article as: Delia Lucarelli , Giacomo Guidali , Roberto Guidotti , Giulia Pieramico , Nadia Bolognini , Gian Luca Romani , Vittorio Pizzella , Laura Marzetti , Pulse waveform and current direction alter network-level TMS-induced functional connectivity: Evidence from TMS-EEG, *NeuroImage* (2026), doi: https://doi.org/10.1016/j.neuroimage.2026.121794

## HIGHLIGHTS

- Pulse waveform and current direction strongly affect TMS-induced functional connectivity.
- TMS parameters shape M1 oscillatory network-level dynamics with frequency-specific patterns.
- Monophasic pulses lead to greater alpha-band connectivity modulations.
- Biphasic AP-PA currents induce the higher connectivity strength in the beta band.
- Recruitment of distinct functional networks could explain variability in TMS effects.

# Pulse waveform and current direction alter network-level TMS-induced functional connectivity: Evidence from TMS-EEG

Delia Lucarelli[1,2,*], Giacomo Guidali[3,*,@], Roberto Guidotti[1,2], Giulia Pieramico[2,4], Nadia Bolognini[3,5], Gian Luca Romani[2], Vittorio Pizzella[1,2,#] & Laura Marzetti[2,4,#,@]

[1] Department of Neuroscience, Imaging and Clinical Sciences, G. D'Annunzio University of Chieti-Pescara, Chieti, Italy

[2] Institute for Advanced Biomedical Technologies, G. D'Annunzio University of Chieti-Pescara, Chieti, Italy

[3] Department of Psychology and Milan Center for Neuroscience - NeuroMI, University of Milano-Bicocca, Milano, Italy

[4] Department of Engineering and Geology, G. D'Annunzio University of Chieti-Pescara, Pescara, Italy

[5] Laboratory of Neuropsychology, IRCCS Istituto Auxologico Italiano, Milano, Italy

**** These authors contributed equally to this work***

***# Shared senior authorship***

**@ Corresponding authors:**

**Dr. Giacomo Guidali, PhD** – giacomo.guidali@unimib.it

Department of Psychology, University of Milano-Bicocca, Piazza dell'Ateneo Nuovo 1, Milano, Italy

**Prof. Laura Marzetti, PhD** – lmarzetti@unich.it

Institute for Advanced Biomedical Technologies, G. D'Annunzio University of Chieti-Pescara, Chieti, Italy

## ABSTRACT

Functional connectivity analyses of electroencephalographic (EEG) data during concurrent transcranial magnetic stimulation (TMS) can offer valuable insight into large-scale network dynamics. Still, the influence of TMS features on these measurements remains poorly understood. This study investigates the impact of key TMS parameters – pulse waveform and current direction – on the induced EEG functional connectivity of the motor system in the alpha and beta frequency bands.

We analyzed data from 32 healthy participants retrieved from an open-access repository. Left primary motor cortex (M1) was stimulated at rest while varying TMS pulse waveform (monophasic, biphasic) and current direction (posterior-to-anterior – PA, anterior-to-posterior – AP). TMS-induced functional connectivity patterns were examined across experimental conditions to assess differences given by the distinct parameters used.

In the alpha-band, TMS-induced left M1 connectivity was associated with a widespread network characterized by right-lateralized (i.e., contralateral to TMS site) communication to sensorimotor regions independent of stimulation features. Beta-band connectivity was more localized, with condition-dependent variations. Monophasic pulses led to stronger connectivity than biphasic pulses in the alpha band, with AP currents inducing the most significant modulation. In biphasic conditions, PA-AP stimulation produced the most substantial connectivity modulation in the alpha-band and the weakest in the beta-band, while AP-PA reversed this pattern.

Our findings highlight that TMS parameters can significantly modulate M1 oscillatory dynamics. The selective activation of distinct functional networks could represent a vital source of variability in TMS applications, emphasizing the importance of carefully choosing TMS features and supporting the evidence that motor system interregional communication follows frequency-specific patterns.


**Keywords:** TMS-EEG, functional connectivity, motor system, current direction, pulse waveform, alpha band, beta band

## 1. INTRODUCTION

Over the past few decades, research has increasingly emphasized that brain functioning depends not only on structural connections but also on the functional organization of large-scale networks (Fries, 2005; Friston, 2011; Siegel et al., 2012; Sporns et al., 2000; Varela et al., 2001; Vidaurre et al., 2018). Functional connectivity has been studied using different non-invasive methods such as functional magnetic resonance imaging (fMRI; van den Heuvel & Hulshoff Pol, 2010), functional near-infrared spectroscopy (fNIRS; Lu et al., 2010), electroencephalography (EEG; Babiloni et al., 2005), and magnetoencephalography (MEG; Marzetti et al., 2019). Correlation-based metrics are mainly used to estimate functional connectivity to infer temporal relationships between brain signals. However, this approach has a methodological limitation: it restricts the ability to draw causal inferences from the observed signals (Fox et al., 2012).

A way to address this constraint is by integrating non-invasive brain stimulation techniques, such as transcranial magnetic stimulation (TMS), which allows for perturbing the ongoing activity of specific brain regions, thereby enabling the causal investigation of their role in network functional organization (Reithler et al., 2011; Siddiqi et al., 2022). Brain imaging has been integrated before, after (i.e., offline), and during (i.e., online) TMS administration. Despite offline TMS protocols have proven informative for refining stimulation targets (Bergmann, Varatheeswaran, et al., 2021; Cao et al., 2024; Cash et al., 2021; Fox et al., 2012) and examining the neurophysiological aftereffects of neuromodulatory interventions (Beynel et al., 2020; Schiena et al., 2021), online approaches, such as TMS-EEG, permit to investigate the immediate neural responses elicited by TMS (Bergmann, Tomasevic, et al., 2021; Hernandez-Pavon et al., 2023; Humaidan et al., 2024; Marzetti et al., 2024; Vetter et al., 2023; Zrenner et al., 2018). EEG (similar to MEG and in contrast to fMRI and fNIRS) enables the investigation of functional connectivity not only as a simultaneous activation of different brain areas but also as a coupling of signals at specific frequencies within short (millisecond-scale) time windows (Marzetti et al., 2019). According to the communication-through-coherence theory, this advantage becomes particularly relevant since the neuronal groups involved in a cognitive function synchronize within a specific frequency band associated with that task (Fries, 2005, 2015). However, the use of TMS-EEG is challenged by the substantial variability in participants' responses to TMS (Corp et al., 2021; Ziemann et al., 2026).

Several studies have highlighted that part of this variability can be attributed to TMS parameters, among which the pulse waveform and the induced current direction, that significantly affect TMS-evoked potentials (TEPs), motor-evoked potentials (MEPs), and behavioral outcomes (Beck, Christiansen, et al., 2024; Bonato et al., 2006; S. Casarotto et al., 2010; Casula et al., 2018, 2022; Guidali et al., 2023; Lucarelli et al., 2025; Sommer et al., 2006, 2013, 2018; Souza et al., 2018). Biophysical modeling studies have linked these effects to the selective engagement of distinct neuronal populations and cortico-cortical circuits (Aberra et al., 2020; Siebner et al., 2022). For instance, TMS pulses delivered over the primary motor cortex (M1) to induce currents in the

precentral gyrus with a posterior-to-anterior (PA) direction preferentially activate neuronal populations located in deeper cortical layers and caudal portions of M1 than the reversed direction (i.e., anterior-to-posterior – AP) that instead is more suitable for activating interconnected cerebral areas (e.g., Lucarelli et al., 2025; Souza et al., 2025; Spampinato, 2020). In this context, TEPs have proven helpful for mapping signal propagation across brain regions (Momi et al., 2023). Yet, it remains an open question whether changes in TMS parameters can systematically affect the recruitment of functional networks.

Despite the potential of TMS-EEG in unveiling large-scale network dynamics, functional connectivity has been scarcely investigated within this framework to date, albeit with promising results (e.g., Bianco et al., 2023; De Martino et al., 2025; Guidali et al., 2025; Luo et al., 2023; Pieramico et al., 2023; Pisoni et al., 2018; Trajkovic et al., 2025; Y. Ye et al., 2022). Since TEPs are generally believed to reflect structural rather than functional brain properties (Momi et al., 2023), they may not be ideal for connectivity analysis. In contrast, induced activity, which is time-locked but not phase-locked to the TMS pulse (Pellicciari et al., 2017), is functionally distinct from evoked activity and is thought to reflect different neural and cognitive mechanisms (Chen et al., 2009, 2012; Federici et al., 2023; Tallon-Baudry, 1999; Yusuf et al., 2017). Specifically, induced responses are hypothesized to represent modulatory, voltage-dependent postsynaptic activity and have been associated with and predictive of TMS aftereffects (Chen et al., 2009; Pellicciari et al., 2017; Veniero et al., 2015). Thus, analyzing source-level functional connectivity of TMS-induced activity may offer a valuable complement to TEP analysis, enabling more profound insight into the dynamic communication between brain areas following stimulation with specific parameters (Chen et al., 2009, 2012).

The present study investigates whether two crucial TMS parameters (Sommer et al., 2023), namely the pulse waveform (monophasic or biphasic) and the induced current direction in the brain (AP or PA), affect TMS-induced EEG functional connectivity of the motor system. It should be noted that throughout the paper, as in our previous works (Guidali et al., 2023; Lucarelli et al., 2025), the current direction (i.e., AP, PA) will always refer to the one induced in the brain relative to the targeted precentral gyrus. For biphasic pulses, the induced direction will refer to the second phase of the stimulation (i.e., ‘biphasic PA’ refers to AP-PA stimulation and ‘biphasic AP’ to PA-AP stimulation), considering that it is thought to induce a stronger neuronal activation than the first phase (Sommer et al., 2023).

In detail, we explored the influence of these two critical TMS parameters in the alpha (8-12 Hz) and beta bands (13-30 Hz), given the pivotal role of these frequency bands in primary motor cortex (M1) activity and inter-areal communication (Groppe et al., 2013; Kilavik et al., 2013; Salmelin & Hari, 1994; van Wijk et al., 2012). We hypothesize that TMS-induced M1 functional connectivity is modulated according to the stimulator’s features, likely with frequency-specific patterns. Our work aims to inform the influence of TMS parameter selection on online and offline targeting of large-scale

functional networks and related oscillatory dynamics, providing a stronger foundation for this class of TMS-EEG analyses.

## 2. MATERIALS and METHODS

### 2.1. Participants

Raw data from the study of Guidali et al. (2023) were utilized (open-access repository: https://gin.g-node.org/Giacomo_Guidali/Guidali_et_al_2023_EJN_RR). The dataset comprises 32 subjects (18 females, mean age ± standard deviation, SD: 27.9 ± 6.9 years; mean education: 16.6 ± 2.9 years). All subjects were right-handed, as assessed using the Edinburgh Handedness Questionnaire (Oldfield, 1971).

The original study (Guidali et al., 2023) adhered to the TMS safety criteria (Rossi et al., 2021) and followed the ethical guidelines outlined in the Declaration of Helsinki. Following the recommendation of the University of Milano-Bicocca's Committee for Research Evaluation, the present study was exempt from ethical approval as it was based on completely anonymized public data provided under a CC-BY-4 license (see the link to the open-access repository reported above).

### 2.2. Experimental procedure

In the original study (Guidali et al., 2023), participants were seated on a chair with their forearms resting on a table. First, after the EEG montage, experimenters identified the participant's right-hand *Abductor Pollicis brevis* (APB) motor hotspot using a biphasic stimulator that induced currents within M1 in the PA direction. The hotspot was used as the stimulation target throughout the whole experiment. Subsequently, the participant underwent seven stimulation blocks, with the order randomized across subjects. In each block, the resting motor threshold (rMT) for that TMS condition was first assessed, followed by delivery of 20 and 80 TMS pulses to record MEPs and TEPs, respectively. TMS intensity was set at 110% of rMT. Stimulation conditions were manipulated by changing the TMS current direction and pulse waveform (Guidali et al., 2023). In the present work, we only considered data from monophasic and biphasic PA and AP TMS-EEG blocks (**Figure 1**). In the original dataset, latero-medial (LM) current direction conditions were also introduced. These directions are not commonly employed in TMS-EEG studies on M1; hence, given the exploratory nature of our work, we have preferred to focus our principal investigation on the current directions (i.e., PA and AP) most frequently used and explored by previous literature (Beck, Heyl, et al., 2024; Corp et al., 2021). Nevertheless, for completeness, functional connectivity patterns in LM conditions were also analyzed and reported in the **Supplemental Analysis S1**.

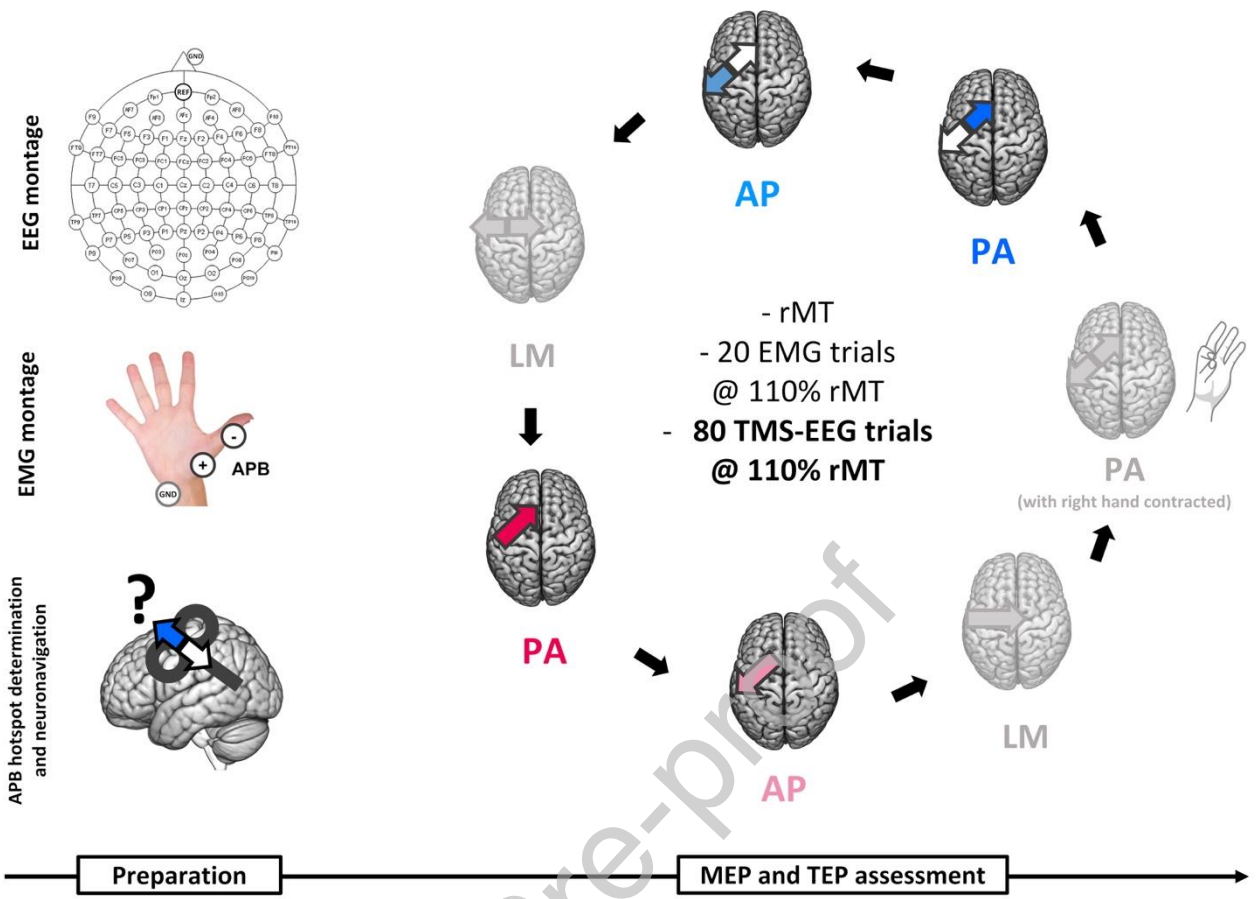


**Figure 1.** Experimental procedure of the original study of Guidali et al. (2023). Participants underwent seven stimulation blocks after completing EEG and EMG setup, neuronavigation, and APB hotspot assessment. Each block featured a unique combination of TMS pulse waveform and current direction and included rMT computation, 20 trials for MEP recording, and 80 trials for suprathreshold TEP recording. Participants observed a fixation cross on a PC screen during MEP and TEP recording. For the present study, blocks involving hand contraction and where TMS was delivered with a latero-medial (LM) direction were excluded from main analyses (blurred in the figure). For completeness, functional connectivity data obtained for LM conditions are reported in the **Supplementary Materials**. We referred the reader to the original work for a detailed description of the original experimental procedure (Guidali et al., 2023). In all figures, colored arrows over left M1 indicate the direction of induced currents in the brain (for biphasic blocks, the condition name referred to the second phase of stimulation, which is indicated by colored arrows; white arrows indicate the first phase).

### 2.3. TMS-EEG recording

EEG activity was recorded using a TMS-compatible amplifier (g.HIamp multichannel amplifier, g.tec medical engineering GmbH) and a 74-channel cap (EasyCap, Brain Products GmbH, Munich, Germany) following the 10-10 system montage, referenced to FPz and with the ground electrode placed on the nose. Skin-electrode impedance was continuously checked and kept below 5 kΩ. The Magstim 200$^2$ and Rapid$^2$ stimulators (Magstim, Whitland, UK) were used for monophasic and biphasic blocks, respectively. The same figure-of-eight coil (Magstim Alpha D70 B.I. Coil Range) was used for the entire experiment. In PA conditions, the coil was oriented 45˚ to the midline, whereas during AP blocks, it was oriented 180˚ to the PA orientation. SofTaxic Optic 3.4 software

(EMS, Bologna, Italy; www.softaxic.com) and related hardware (Polaris Spectra, NDI, Waterloo, Canada) monitored the correct coil positioning. During TMS-EEG, the Inter-Stimulus Interval (ISI) was jittered between 4 and 6 seconds. White noise was played through noise-canceling earphones during each block to mask the TMS click (Biabani et al., 2019). Data was sampled at 9.6 kHz. MATLAB scripts (MATLAB R2020b, The MathWorks, Natick, MA, USA) controlling blocks' randomization, TMS timing, and EEG triggers are available at https://gin.g-node.org/Giacomo_Guidali/Guidali_et_al_2023_EJN_RR/src/master/Script%20task.

### 2.4. EEG preprocessing

To preprocess the data, we adapted the pipeline available at https://gin.g-node.org/Giacomo_Guidali/Guidali_et_al_2023_EJN_RR/src/master/Script%20preprocessing%20EMG-EEG/preprocessingTEP_pipeline.m. It consists of a MATLAB script using EEGLAB (v.2024; Delorme & Makeig, 2004) and Fieldtrip (v.20240416; Oostenveld et al., 2011) toolboxes.

In detail, we performed the following steps: signal interpolation around the TMS pulse (-1 to 2 ms), high-pass filtering (1 Hz), data down-sampling to 4.8 kHz, and data epoching from -1 to 1 s. Then, we adopted the Source-estimate-Utilizing Noise-Discarding (SOUND) algorithm to attenuate extracranial noise from noisy channels (spherical-head-3-layer model for the lead-field matrix and regularization of $\lambda = .1$ - Mutanen et al., 2018). Trials with EEG exceeding 5 SD were automatically excluded from further analysis. We performed independent component analysis (ICA; fastICA algorithm – Hyvärinen & Oja, 2000)to identify and remove ocular artifacts. ICA was also used to remove residual electrode decay artifacts, particularly prominent in some participants during monophasic stimulation (Guidali et al., 2023). Muscular artifacts were removed within the first 50 ms using the source-informed reconstruction (SSP-SIR) algorithm (Mutanen et al., 2016). Finally, we baseline-corrected the data between -200 and -5 ms, ran a second manual artifact rejection, applied a low-pass filter (70 Hz) and a notch filter (49-51 Hz). The grand average across all trials was computed for each block (i.e., stimulation condition) using the Fieldtrip toolbox (**Supplemental Figure S3**; pre-processing information is reported in **Supplemental Table S3**). Then, the grand average signal was subtracted from each trial within each block to remove the evoked signal and unveil the induced activity. Lastly, the data was downsampled to 250 Hz.

### 2.5. Source estimation

To visually inspect the spectral characteristics of the induced signal, time-frequency analysis was performed for the four stimulation conditions, and the resulting plots are shown in the **Supplemental Figure S4**. We used standard brain models implemented in Fieldtrip to estimate source activity. A boundary-element method (BEM) model was used as the forward model with standard electrode positions. The 7.5 mm source model grid was used as a template to create a source model linearly warped to the MRI template (2 mm isotropic resolution). The lead-field matrix was computed, and

source activity was estimated using the standardized low-resolution brain electromagnetic tomography (sLORETA) algorithm (Pascual-Marqui, 2002). To facilitate the interpretation of the results and to reduce data dimensionality, source activity was parceled into 90 cerebral regions using the AAL atlas (Tzourio-Mazoyer et al., 2002), and principal component analysis (PCA) was performed for each parcel.

### 2.6. Functional connectivity analysis

We performed functional connectivity analysis using the debiased weighted phase lag index (dwPLI; Vinck et al., 2011) between the signals resulting from the PCA within each parcel, considering the stimulated area (M1 – corresponding to the left precentral gyrus parcel, lpM1) as the seed parcel and the other 89 as target parcels. Importantly, dwPLI-based metrics have already been successfully applied to TMS-EEG data to investigate functional connectivity (e.g., De Martino et al., 2025; Guidali et al., 2025; Trajkovic et al., 2025; L. Ye et al., 2025). We filtered the entire epoch in the alpha and beta frequency bands using a 38-order finite impulse response (FIR) filter, and the Hilbert transform was applied. Specifically, we used an 8-12 Hz filter for the alpha band and a 13-30 Hz filter for the beta band. The -700 to -315 ms time interval was considered the 'pre-TMS' window, and the 15 to 400 ms one was identified as the 'post-TMS' window. For both windows, the dwPLI was computed for each trial, and connectivity values were averaged across trials of the same block.

### 2.7. Statistical analysis

First, we tested possible differences in lpM1 connectivity during the pre-TMS period in alpha and beta bands as a quality check to assess that no connectivity differences occurred in the pre-TMS window among the different stimulation conditions – given that participants were always at rest with their eyes open. To this aim, for each subject and condition, we computed an index of mean connectivity strength, calculating the mean dwPLI between lpM1 and all other 89 parcels and comparing them between experimental conditions with a 'Pulse waveform' (monophasic, biphasic) X 'Current direction' (AP, PA) repeated-measures analysis of variance (rmANOVA). These analyses showed no statistically significant interactions, suggesting that lpM1 mean connectivity at rest was comparable in all our experimental conditions (all $F$s < 1.91, all $p$s > .177, **Supplemental Figure S5**). Then, we performed parcel-wise paired-samples t-tests (two-tailed) on pre-TMS and post-TMS dwPLI for each stimulation condition and subject to detect which parcels showed significant changes in lpM1-induced functional connectivity after TMS. This pruning step is indeed vital to further account for spurious functional connectivity (Marzetti et al., 2019; Schoffelen & Gross, 2009; Vinck et al., 2011), avoiding possible over-interpretation of connectivity patterns across parcels and experimental conditions (Bastos & Schoffelen, 2016; Gross et al., 2013). Hence, only parcels showing a significant pre-post modulation of dwPLI values, indicating lpM1 connectivity changes likely induced by the TMS pulse, were considered in the following analyses.

To quantitatively explore differences in TMS-induced connectivity, we computed, for each band of interest, (i) the *connectivity strength*, an index of the strength of left M1 large-scale connectivity profile (Guidali et al., 2025), by summing the dwPLI values of all the significant parcels found statistically different from baseline and (ii) the *mean connectivity strength*, an index of the mean strength of left M1 connectivity profile, by dividing the *connectivity strength* for the number of parcels considered. Possible differences in these indices were explored with 'Pulse waveform' (monophasic, biphasic) X 'Current direction' (AP, PA) rmANOVAs.

We set the statistical significance threshold at $p < .05$ for all analyses. We confirmed the normality of all our distributions by checking them with the Shapiro-Wilk test and Q-Q plots assessment. In rmANOVAs, statistically significant effects were deepened with post-hoc tests applying the Bonferroni correction for multiple comparisons. Partial eta-squared ($\eta_p^2$) and Cohen's *d* were reported as effect size values for rmANOVAs and t-tests, respectively. Statistical analyses were performed using the software Jamovi (The Jamovi Project, 2025).

## 3. RESULTS

### 3.1. TMS-induced connectivity modulations in the alpha band

All parcels showing a significant connectivity modulation with the left M1 in the post-TMS compared to the pre-TMS interval are reported in **Tables 1** and **2.** Regardless of the stimulation condition, TMS over left M1 modulated alpha-band functional connectivity with the contralateral precentral, postcentral, and superior parietal gyri. Using monophasic PA waveforms strongly modulated lpM1 connectivity with fronto-orbital regions of the left hemisphere, right parietal areas (as the inferior parietal, supramarginal, and angular gyri), and the supplementary motor area (SMA) of both hemispheres. In contrast, monophasic AP stimuli selectively modulated lpM1 connectivity with right frontal areas (including the dorsolateral prefrontal cortex and the cingulum), left occipital regions, and bilateral inferior parietal gyri. Furthermore, this condition selectively influenced lpM1 connectivity with the ipsilateral inferior parietal gyrus, but not with the contralateral homologous parcel, which, instead, was modulated in all the other experimental conditions. Considering biphasic waveforms, PA currents were the only ones modulating targeted M1 communication with the ipsilateral postcentral gyrus and the contralateral parietal regions, closely resembling those influenced by the homolog monophasic condition. Lastly, the biphasic AP condition engaged the contralateral SMA, left occipital areas, and right-lateralized parietal regions comprising the inferior parietal gyrus and the angular gyrus (**Figure 2**).

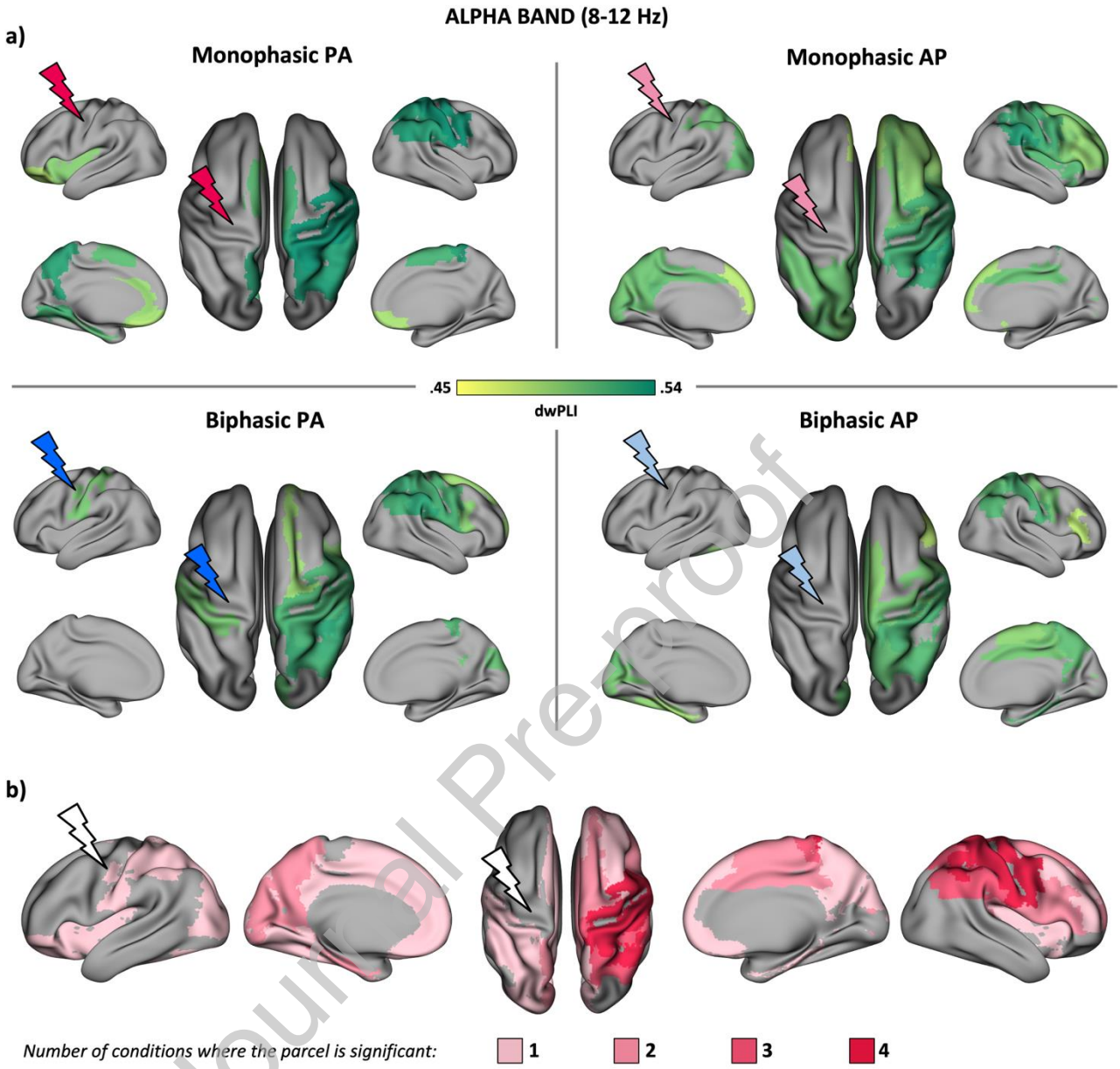


**Figure 2. a)** Alpha-band dwPLI values of the parcels that showed a significant connectivity modulation with the left precentral parcel in the post-TMS interval, displayed on the inflated brain template. **b)** Overlap of the parcels showing a significant connectivity modulation in the alpha band across the four experimental conditions. Lightning (red: monophasic PA, light red: monophasic AP, blue: biphasic PA, light blue: biphasic AP) indicates the site of TMS (i.e., left M1).

The rmANOVA on the *connectivity strength* index revealed a significant effect of factors 'Pulse waveform' ($F_{1,31} = 1726.15$, $p < .001$, $\eta_p^2 = .98$), 'Current direction' ($F_{1,31} = 165.17$, $p < .001$, $\eta_p^2 = .84$) and, crucially, of their interaction ($F_{1,31} = 8.09$, $p = .008$, $\eta_p^2 = .21$). Post-hoc comparisons showed that monophasic conditions ($PA_{monophasic}$: 13.25 ± .28; $AP_{monophasic}$: 14.17 ± .32) induced higher *connectivity strength* values than biphasic ones ($PA_{monophasic}$ *vs.* $PA_{biphasic}$: 6.67 ± .15, $t_{31} = 40.72$, $p_{Bonf} < .001$, $d = 7.2$; vs. $AP_{biphasic}$: 8.06 ± .18, $t_{31} = 33.19$, $p_{Bonf} < .001$, $d = 5.87$; $AP_{monophasic}$ *vs.* $PA_{biphasic}$: $t_{31} = 32.92$, $p_{Bonf} < .001$, $d = 5.82$; vs. $AP_{biphasic}$: $t_{31} = 38.35$, $p_{Bonf} < .001$, $d = 6.78$). Furthermore, AP

currents led to higher values than PA ones for both monophasic ($t_{31}$ = 6.02, $p_{Bonf}$ < .001, $d$ = 1.06) and biphasic waveforms ($t_{31}$ = 16.69, $p_{Bonf}$ < .001, $d$ = 2.95; **Figure 3a**).

Considering the *mean connectivity strength* index, rmANOVA showed a significant interaction 'Pulse waveform' X 'Current direction' ($F_{1,31}$ = 17.39, $p$ < .001, $\eta_p^2$ = .36). Main factors reached significance too ('Pulse waveform': $F_{1,31}$ = 19.19, $p$ < .001, $\eta_p^2$ = .39; 'Current direction': $F_{1,31}$ = 9.66, $p$ = .004, $\eta_p^2$ = .24). Interestingly, post-hoc comparisons revealed that biphasic PA currents induced the weakest *mean connectivity strength* (.476 ± .01 *vs.* $PA_{monophasic}$: .51 ± .011, $t_{31}$ = -6.84, $p_{Bonf}$ < .001, $d$ = -1.21; $AP_{monophasic}$: .506 ± .011, $t_{31}$ = -6.02, $p_{Bonf}$ < .001, $d$ = -1.06; $AP_{biphasic}$: .504 ± 011, $t_{31}$ = -5.32, $p_{Bonf}$ < .001, $d$ = -0.94;) with no differences among the other three experimental conditions (all ts < 1.02; all *p*s > .99, **Figure 3b**).

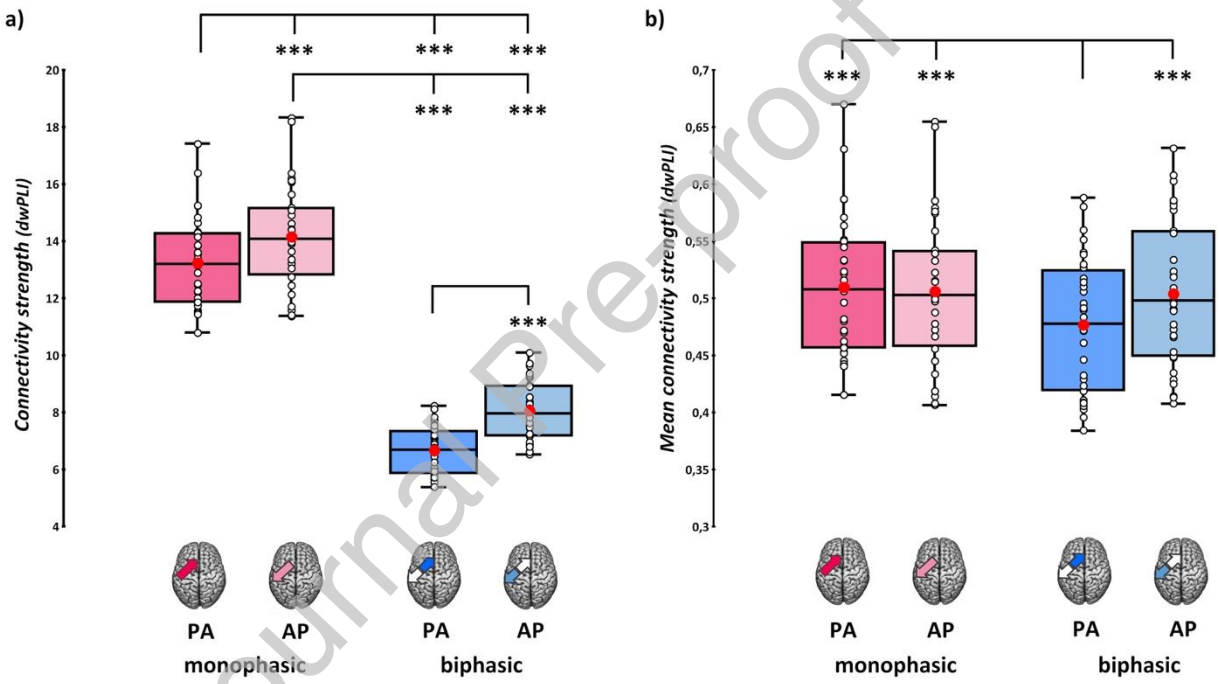


**Figure 3.** Connectivity strength (**a**) and mean connectivity strength (**b**) indexes for the alpha band in the four experimental conditions (red: monophasic PA, light red: monophasic AP, blue: biphasic PA, light blue: biphasic AP). In the box-and-whiskers plots, red dots indicate the means of the distributions. The center line reports their median values. White dots show single-subject scores. The box contains the 25$^{th}$ to 75$^{th}$ percentiles of the dataset. Whiskers extend to the largest observation falling within the 1.5 * inter-quartile range from the first/third quartile. Significant Bonferroni-corrected post-hoc comparisons are reported (*** = p < .001).

### 3.2. TMS-induced connectivity modulations in the beta band

All parcels showing a significant connectivity modulation with the left M1 in the post-TMS compared to the pre-TMS interval are reported in **Tables 3** and **4**. Overall, TMS-induced modulations in the beta band affected fewer parcels than those in the alpha band. Biphasic PA currents induced connectivity changes involving the greatest network of regions. This condition affected the lpM1's

functional connectivity with frontal areas, including the contralateral precentral gyrus, SMA, and, bilaterally, the posterior cingulate cortex. Furthermore, it influenced lpM1 connectivity with right occipital regions, the left superior parietal gyrus, and both hemispheres' inferior temporal gyri and precuneus. In contrast, connectivity changes induced by biphasic AP currents were limited to fewer regions, involving subcortical or deeper parcels, such as the right hemisphere insula and the amygdala, or the left hemisphere cuneus and precuneus. Considering monophasic waveforms, lpM1 connectivity modulations induced by PA currents are concerned with a more restricted network than the ones induced by the opposite current direction (i.e., AP). Indeed, they mainly encompassed the right postcentral gyrus, posterior cingulum, and left hippocampal regions. AP currents, on the other side, elicited right-lateralized connectivity modulations with contralateral orbito-frontal, parietal (i.e., superior parietal and angular gyri), and occipital areas, as well as with the middle frontal and temporal gyri of the left hemisphere (**Figure 4**).

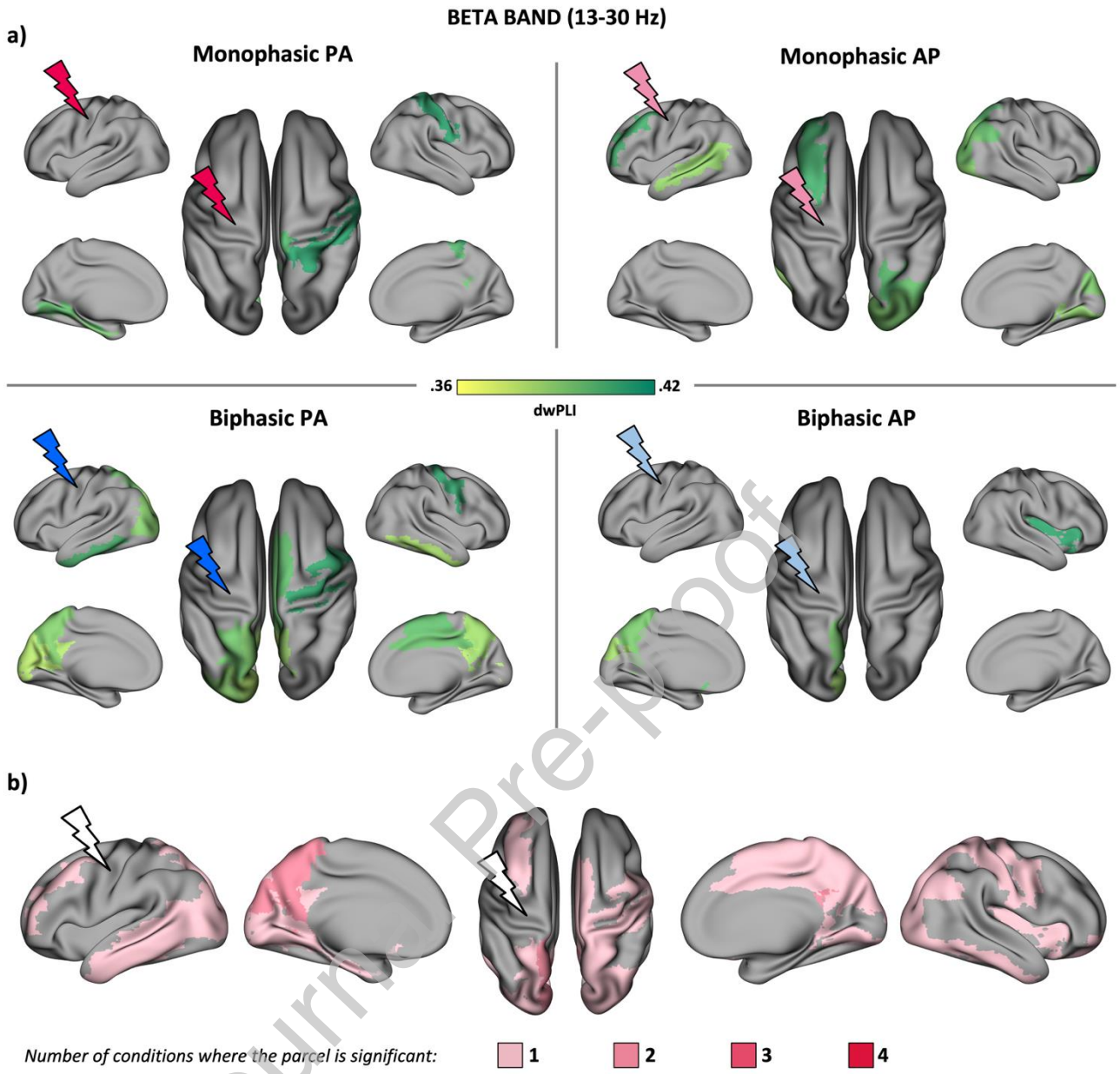




**Figure 4. a)** Beta-band dwPLI values of the parcels that showed a significant connectivity modulation with the left precentral parcel in the post-TMS interval, displayed on the inflated brain template. **b)** Overlap of the parcels showing a significant connectivity modulation in the beta band across the four experimental conditions. Lightning (red: monophasic PA, light red: monophasic AP, blue: biphasic PA, light blue: biphasic AP) indicates the site of TMS (i.e., left M1).

The rmANOVA on the induced *connectivity strength* index confirmed these patterns, highlighting a significant 'Pulse waveform' X 'Current direction' interaction ($F_{1,31} = 2312$, $p < .001$, $\eta_p^2 = .99$), as well as significant main effects of both factors ('Pulse waveform': $F_{1,31} = 1158$, $p < .001$, $\eta_p^2 = .97$; 'Current direction': $F_{1,31} = 395$, $p < .001$, $\eta_p^2 = .93$). Post-hoc comparisons revealed that using biphasic PA currents led to the highest *connectivity strength* values (5.85 ± .06 *vs.* $PA_{monophasic}$: 3.2 ± .04, $t_{31} = 54.28$, $p_{Bonf} < .001$, $d = 9.6$; $AP_{monophasic}$: 4.33 ± .05, $t_{31} = 32.19$, $p_{Bonf} < .001$, $d = 5.69$; $AP_{biphasic}$: 3.22 ± .03, $t_{31} = 44.45$, $p_{Bonf} < .001$; $d = 7.86$). Moreover, monophasic AP stimulation led to higher values

than biphasic AP ($t_{31}$ = 27.28, $p_{Bonf}$ < .001, $d$ = 4.82) and monophasic PA conditions ($t_{31}$ = 23.49, $p_{Bonf}$ < .001, $d$ = 4.15) with no differences occurring between the latter ones ($t_{31}$=.02, $p_{Bonf}$=.99, $d$=.08; **Figure 5a**).

The rmANOVA on *mean connectivity strength* values showed only a significant interaction effect ($F_{1,31}$ = 5.77, $p$ = .022, $\eta_p^2$ = .16). However, post-hoc comparisons did not show any condition significantly differing from another, suggesting that *mean connectivity strength* values in the beta-band were similar for all our experimental conditions. Likely, the interaction effect was driven by a lower *mean connectivity strength* when biphasic PA currents were used (.39 ± .004) compared to monophasic PA (.4 ± .004) and biphasic AP conditions (.402 ± .004), as highlighted when we ran planned comparisons between these conditions ($PA_{biphasic}$ *vs.* $PA_{monophasic}$: $t_{31}$ = -2.32, $p$ = .027, $d$ = -.41; *vs.* $AP_{biphasic}$: $t_{31}$ = -2.4, $p$ = .022, $d$ = -.43; **Figure 5b**). Main effect of 'Pulse waveform' ($F_{1,31}$ = .28, $p$ < .60, $\eta_p^2$ = .009) and 'Current direction' ($F_{1,31}$ = .961, $p$ = .334, $\eta_p^2$ = .03) did not reach statistical significance.

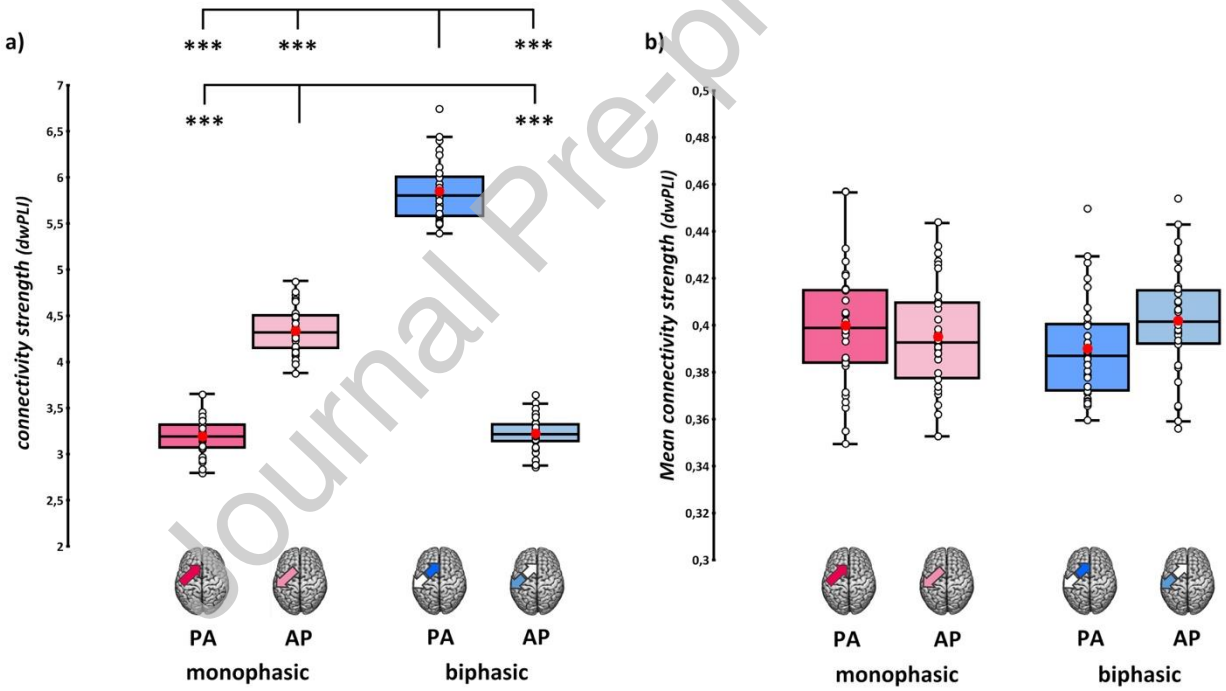


**Figure 5.** Connectivity strength (**a**) and mean connectivity strength (**b**) indexes for the beta band in the four experimental conditions (red: monophasic PA, light red: monophasic AP, blue: biphasic PA, light blue: biphasic AP). In the box-and-whiskers plots, red dots indicate the means of the distributions. The center line reports their median values. White dots show single-subject scores. The box contains the 25$^{th}$ to 75$^{th}$ percentiles of the dataset. Whiskers extend to the largest observation falling within the 1.5 * inter-quartile range from the first/third quartile. Significant Bonferroni-corrected post-hoc comparisons are reported (*** = p < .001).

## 4. DISCUSSION

The present work aims to elucidate the influence of key TMS technical parameters, namely pulse waveform and current direction, on stimulation-induced functional connectivity patterns within the motor system. Our findings suggest that altering the TMS pulse waveform and the direction of tissue-induced currents can significantly modulate the network-level dynamics of M1, exhibiting distinct frequency-specific patterns. This corroborates the evidence that motor system communication in the alpha and beta bands follows different interregional dynamics, likely conveying complementary aspects of cortical elaboration (Stolk et al., 2019; van Wijk et al., 2012).

### 4.1. Different effects of TMS parameters on alpha- and beta-band-induced connectivity

Overall, left M1 Connectivity modulation in the alpha band appears to involve a broader network, with greater right-lateralized communication to sensorimotor regions across stimulation conditions. Conversely, induced M1 communication is less widespread in the beta band, with regional patterns varying across conditions. Our evidence aligns with the literature, which shows that slower rhythms, in contrast to faster activity, reflect the coordination of multiple areas corresponding to wider networks (Athanasiou et al., 2018; Chapeton et al., 2019). In the alpha band, monophasic pulses caused greater connectivity strength than biphasic ones, with monophasic AP currents inducing the strongest connectivity modulation and biphasic PA inducing the weakest. Interestingly, alpha-band synchronization induced by this latter condition is also the lowest at the mean connectivity level. Critically, beta-band connectivity followed a distinct pattern. Here, biphasic PA stimulation induced higher connectivity strength, though significant modulations did not accompany it at the mean connectivity level. Thus, biphasic PA was the most effective condition in modulating the left M1 connectivity profile in the beta band but the least effective in the alpha band.

The distinct patterns observed in alpha and beta frequencies can be attributed to the functional dissociation of these rhythms within the motor system. Indeed, alpha activity is associated with the inhibition of task-irrelevant regions and sensory feedback processing, while beta-band oscillations relate more strictly to motor control and sensorimotor integration (Brinkman et al., 2014, 2016; Haegens, Nácher, Hernández, et al., 2011; Haegens, Nácher, Luna, et al., 2011; Palva & Palva, 2011; Stolk et al., 2019). Moreover, these two rhythms are generated in different sensorimotor regions: alpha activity originates in the postcentral gyrus and beta activity in the precentral one (Stolk et al., 2019; van Wijk et al., 2012). Alpha- and beta-band functional dissociation was also observed in TMS studies. For instance, MEPs with the highest amplitude are elicited at opposite phases of alpha and beta rhythms, specifically at the trough for alpha and at the peak for beta (Wischnewski et al., 2022). Also, corticomuscular coherence in the alpha and beta bands before TMS has the opposite relation with MEP amplitude (i.e., MEPs were smaller when preceded by high pre-TMS

beta-band power and low alpha-band corticomuscular coherence, and vice versa; Schulz et al., 2014).

Our findings corroborate that changing the current direction and pulse waveform influences the neuronal populations targeted by TMS (Aberra et al., 2020). Single-pulse TMS affects spontaneous brain activity in the targeted area and its connected regions (Momi et al., 2021; Pellicciari et al., 2017). Therefore, changes in induced connectivity patterns are likely due to the activation of distinct neuronal populations, which, when stimulated, modulate their functional coupling with interconnected regions.

### 4.2. TMS-induced connectivity as a valuable proxy for neuromodulatory effects

The neurophysiological substrates of these results are not easily disentangled, considering that, unlike evoked potentials, induced activity has been poorly investigated within the TMS-EEG framework.

Induced responses can be attributed to the TMS modulatory effects (Pellicciari et al., 2017; Veniero et al., 2015). Indeed, neuronal connections associated with induced activity are thought to spread across supra-granular layers, which are primarily populated by NMDA and metabotropic glutamate receptors, a class of receptors strictly related to modulatory voltage-dependent postsynaptic effects grounding cortical plasticity (Anwyl, 1999; Chen et al., 2009; Eaton & Salt, 1996; Hunt & Castillo, 2012). This evidence makes our results more comparable to modulations observed after neuromodulatory protocols.

Within this framework, many studies investigated how stimulation parameters affect repetitive TMS (rTMS) outcomes, focusing on corticospinal excitability as the principal neurophysiological variable (Arai et al., 2005; Di Lazzaro et al., 2011; Hamada et al., 2012; Sommer et al., 2013; Suppa et al., 2008; Talelli et al., 2007) and often using biphasic waveforms due to lower energy demands (Sommer et al., 2023). Our results demonstrate that biphasic (PA-)AP stimulation induces the strongest network-level connectivity modulation (i.e., *connectivity strength* index) in the alpha band and the weakest in the beta band, whereas (AP-)PA stimulation produces the opposite pattern. Considering the neuronal population preferentially targeted by PA and AP currents (Aberra et al., 2020; Siebner et al., 2022), we propose that the pattern of results found for biphasic waveforms may reflect the greater effectiveness of the first phase of stimulation in driving TMS-induced connectivity. Our claim is supported by prior literature that aligns well with the significant modulations observed in our data, at least for biphasic conditions.

In the first place, previous neuromodulatory studies have demonstrated that AP currents more effectively stimulate the superficial layers of M1, whereas PA currents more easily reach the deeper layers (A. Casarotto et al., 2023; Koch et al., 2013; Sommer et al., 2013). Interneurons involved in cortico-cortical communication and network-wide activation are more abundant in M1's superficial layers. In contrast, deeper layers are primarily populated by neurons that directly activate the

pyramidal tract (Harris & Shepherd, 2015; Weiler et al., 2008). Hence, at least structurally, AP stimulation could be more effective in directly activating cortico-cortical interneurons and, in turn, cortical regions interconnected with M1 (Lucarelli et al., 2025). Considering the findings of the present work, in the beta band, biphasic (AP-)PA was the only condition that modulated the connectivity of the stimulated M1 with the contralateral precentral gyrus and the supplementary motor area, in contrast to (PA-)AP. This latter condition induced less widespread modulation; therefore, we hypothesize that it maximizes its modulatory effects on local intra-areal dynamics. In this vein, a recent study demonstrated that, after biphasic (AP-)PA rTMS over M1, M1 stimulation evoked an increase of phase coherence in the beta band within the contralateral hemisphere (De Martino et al., 2025), i.e., a topographical pattern closely resembling the one observed here for TMS-induced connectivity using the same combination of parameters. This evidence is further corroborated by the literature investigating how changes in technical parameters during rTMS administration affect its aftereffects. Previous studies show that administering rTMS over M1 with biphasic pulses inducing (PA-)AP currents is the most effective set of parameters for modulating MEP amplitude (Di Lazzaro et al., 2011; Halawa et al., 2019; Sommer et al., 2013, 2018, 2023; Talelli et al., 2007) and amplitude/latency of an earlier TEP component (i.e., N15; Kanig et al., 2025) that likely reflects the direct activation of M1 (Farzan & Bortoletto, 2022). Conversely, (AP-)PA direction influences neurophysiological and behavioral markers of contralateral motor system activity, indicating more cortical widespread effects after rTMS administration (Shirota et al., 2017; Suppa et al., 2008).

Secondly, as already mentioned, sensorimotor alpha rhythms are thought to arise from cortical generators located primarily in the postcentral gyrus (Stolk et al., 2019; van Wijk et al., 2012), and TMS pulses inducing PA currents activate more effectively caudal regions of the motor cortex, which are densely interconnected with the somatosensory cortex (Siebner et al., 2022). On the contrary, beta rhythms originate from cortical generators located more anteriorly (Jensen et al., 2005; van Wijk et al., 2012), and AP currents are thought to preferentially activate the rostral part of the precentral gyrus (Siebner et al., 2022), potentially making them more suitable for modulating oscillatory dynamics in this higher band. According to this framework, our findings show that biphasic pulses where the first stimulation phase was delivered in the PA direction [i.e., (PA-)AP condition] led to greater network-level connectivity modulation in the alpha band than the reversed direction [i.e., (AP-)PA], with the opposite pattern for the beta band. Hence, this evidence further suggests that the first stimulation phase of biphasic stimulation better frames induced connectivity patterns.

Nevertheless, it is essential to highlight that biphasic modulations likely reflect the intertangled effects induced by both stimulation phases (Sommer et al., 2018, 2023), and this could explain why their patterns are not superimposable to monophasic ones, especially in the alpha band, where monophasic PA stimulation is less effective than AP one. Furthermore, we point out that the hypothesis that the first phase of biphasic stimulation could be more effective for influencing M1

functional connectivity is somewhat in contrast with previous MEP and modeling studies, which suggest that the second phase of biphasic pulses is indeed the most effective one for neuronal activation (e.g., Aberra et al., 2020; Corthout et al., 2001; Menon et al., 2023; Sommer et al., 2006, 2018). Still, all these studies focused their investigation on TMS-evoked cortical/corticospinal reactivity and, therefore, explored a different variable than our study, which focused on TMS-induced large-scale oscillatory dynamics.

However, given the exploratory nature of the present investigation, further studies are needed to better disentangle the current direction patterns found for biphasic conditions.

### 4.3. Future directions and limitations

The current findings open up important methodological and thought-provoking considerations. Our data suggest that the TMS pulse waveform and current direction have a considerable impact on the functional connectivity induced within the motor system, likely greater than that reported for M1-TEP components derived from the same dataset (Guidali et al., 2023; Lucarelli et al., 2025). Supplemental analyses conducted for the LM current direction conditions of the original dataset (Guidali et al., 2023) further corroborate this evidence. As reported in the **Supplemental Analysis S1**, employing stimulation parameters (i.e., LM) that previous MEP literature has shown as optimal for the direct activation of the corticospinal tract's pyramidal neurons (Di Lazzaro et al., 2012, 2018), and that seem not to impact TEP spatiotemporal features (Guidali et al., 2023; Lucarelli et al., 2025), drastically reduces the strength and the spread of TMS-induced M1 oscillatory activity in both frequency bands. Overall, it appears that TMS-induced functional connectivity likely involves neuronal populations that are partially distinct from those responsible for TMS-evoked effective connectivity. From a broader perspective, this aspect may be crucial for the variability of TMS aftereffects between and within studies. Hence, evidence that different TMS parameters have a significant impact on network-level functional connectivity could provide valuable insights, guiding future studies to selectively target distinct neural circuits and reveal specific functional patterns.

Regardless of the specific neuronal substrate, our results emphasize the importance of carefully selecting stimulation parameters in TMS-EEG studies to minimize methodological confounding. In the future, this investigation could be extended beyond M1, e.g., to brain areas commonly targeted in plasticity-inducing TMS protocols (Asgarinejad et al., 2024; Fitzsimmons et al., 2024; Li et al., 2024), thus relating better the induced connectivity, neuromodulatory effects, and the influence of TMS parameters. Tools such as the multi-locus TMS (Koponen et al., 2018; Nieminen et al., 2022; Sinisalo et al., 2024; Souza et al., 2025) will be pivotal for precisely manipulating stimulation features and better deepening these aspects.

The current study has some limitations that should be considered when interpreting the results. In the original work (Guidali et al., 2023), two distinct TMS devices delivered monophasic and biphasic stimulation. Therefore, some technical differences associated with the stimulator cannot be fully

controlled, which may weaken comparisons between monophasic and biphasic conditions. Moreover, the subjects' structural MRI data and EEG cap digitalization were unavailable, which reduced the accuracy of the source estimation. Finally, changing the current direction and, consequently, the coil orientation, can lead to different somatosensory and auditory experiences across conditions, affecting cortical elaboration and the recorded TEPs (Biabani et al., 2019). However, it is worth noting that participants in the original experiment did not report significant TMS-related sensory differences across stimulation conditions, as presented in Supplemental Figure 3 of Lucarelli et al.'s work, which used the same dataset as the present study (Lucarelli et al., 2025).

## 5. CONCLUSION

Our study demonstrates that TMS parameters, specifically pulse waveform and current direction, significantly influence TMS-induced functional connectivity, exhibiting frequency- and condition-specific modulations. These findings indicate that different TMS parameters can activate distinct functional networks related to the stimulated M1, highlighting the critical importance of carefully selecting stimulation parameters in TMS studies that explore (and exploit) functional connectivity.

**FUNDING**

This work was supported by the European Research Council (ERC Synergy) under the European Union's Horizon 2020 research and innovation programme (ConnectToBrain; grant agreement No. 810377). The content of this article reflects only the author's view, and the ERC Executive Agency is not responsible for the content. GG and NB were supported by the PRIN Grant '2022-NAZ-0168' from the Italian Ministry of University and Research.

**COMPETING INTERESTS**

The authors declare that the research was conducted without any commercial or financial relationships that could be construed as a potential conflict.

**DATA AVAILABILITY**

Raw data can be found at: https://gin.g-node.org/Giacomo_Guidali/Guidali_et_al_2023_EJN_RR. The database and statistical analyses of the present study are available on the Open Science Framework (OSF) at https://osf.io/8z4rb.

**CRediT AUTHORS' CONTRIBUTION**

**Delia Lucarelli**: conceptualization, methodology, software, investigation, formal analysis, visualization, writing – original draft

**Giacomo Guidali**: conceptualization, methodology, investigation, formal analysis, data curation, visualization, writing – original draft

**Roberto Guidotti**: software, visualization, writing – review & editing

**Giulia Pieramico:** software, writing – review & editing

**Nadia Bolognini:** funding acquisition, writing – review & editing

**Gian Luca Romani:** resources, funding acquisition, writing– review & editing.

**Vittorio Pizzella:** conceptualization, methodology, supervision, resources, funding acquisition, writing– review & editing.

**Laura Marzetti:** conceptualization, methodology, supervision, resources, funding acquisition, writing– review & editing.

## REFERENCES


Aberra, A. S., Wang, B., Grill, W. M., & Peterchev, A. V. (2020). Simulation of transcranial magnetic stimulation in head model with morphologically-realistic cortical neurons. *Brain Stimulation*, *13*(1), 175–189. https://doi.org/10.1016/J.BRS.2019.10.002

Anwyl, R. (1999). Metabotropic glutamate receptors: electrophysiological properties and role in plasticity. *Brain Research Reviews*, *29*(1), 83–120. https://doi.org/10.1016/S0165-0173(98)00050-2

Arai, N., Okabe, S., Furubayashi, T., Terao, Y., Yuasa, K., & Ugawa, Y. (2005). Comparison between short train, monophasic and biphasic repetitive transcranial magnetic stimulation (rTMS) of the human motor cortex. *Clinical Neurophysiology*, *116*(3), 605–613. https://doi.org/10.1016/j.clinph.2004.09.020

Asgarinejad, M., Saviz, M., Sadjadi, S. M., Saliminia, S., Kakaei, A., Esmaeili, P., Hammoud, A., Ebrahimzadeh, E., & Soltanian-Zadeh, H. (2024). Repetitive transcranial magnetic stimulation (rTMS) as a tool for cognitive enhancement in healthy adults: a review study. *Medical & Biological Engineering & Computing*, *62*(3), 653–673. https://doi.org/10.1007/s11517-023-02968-y

Athanasiou, A., Klados, M. A., Styliadis, C., Foroglou, N., Polyzoidis, K., & Bamidis, P. D. (2018). Investigating the Role of Alpha and Beta Rhythms in Functional Motor Networks. *Neuroscience*, *378*, 54–70. https://doi.org/10.1016/j.neuroscience.2016.05.044

Babiloni, F., Cincotti, F., Babiloni, C., Carducci, F., Mattia, D., Astolfi, L., Basilisco, A., Rossini, P. M., Ding, L., Ni, Y., Cheng, J., Christine, K., Sweeney, J., & He, B. (2005). Estimation of the cortical functional connectivity with the multimodal integration of high-resolution EEG and fMRI data by directed transfer function. *NeuroImage*, *24*(1), 118–131. https://doi.org/10.1016/j.neuroimage.2004.09.036

Bastos, A. M., & Schoffelen, J. M. (2016). A tutorial review of functional connectivity analysis methods and their interpretational pitfalls. In *Frontiers in Systems Neuroscience* (Vol. 9, Issue JAN2016). Frontiers Research Foundation. https://doi.org/10.3389/fnsys.2015.00175

Beck, M. M., Christiansen, L., Madsen, M. A. J., Jadidi, A. F., Vinding, M. C., Thielscher, A., Bergmann, T. O., Siebner, H. R., & Tomasevic, L. (2024). Transcranial magnetic stimulation of primary motor cortex elicits an immediate transcranial evoked potential. *Brain Stimulation*, *17*(4), 802–812. https://doi.org/10.1016/j.brs.2024.06.008

Beck, M. M., Heyl, M., Mejer, L., Vinding, M. C., Christiansen, L., Tomasevic, L., & Siebner, H. R. (2024). Methodological Choices Matter: A Systematic Comparison of TMS-EEG Studies Targeting the Primary Motor Cortex. *Human Brain Mapping*, *45*(15). https://doi.org/10.1002/hbm.70048

Bergmann, T. O., Tomasevic, L., & Siebner, H. R. (2021). Transcranial brain stimulation and EEG/MEG. *The Oxford Handbook of Transcranial Stimulation*, 741–778. https://doi.org/10.1093/OXFORDHB/9780198832256.013.26

Bergmann, T. O., Varatheeswaran, R., Hanlon, C. A., Madsen, K. H., Thielscher, A., & Siebner, H. R. (2021). Concurrent TMS-fMRI for causal network perturbation and proof of target engagement. *NeuroImage*, *237*. https://doi.org/10.1016/j.neuroimage.2021.118093

Beynel, L., Powers, J. P., & Appelbaum, L. G. (2020). Effects of repetitive transcranial magnetic stimulation on resting-state connectivity: A systematic review. *NeuroImage*, *211*. https://doi.org/10.1016/j.neuroimage.2020.116596

Biabani, M., Fornito, A., Mutanen, T. P., Morrow, J., & Rogasch, N. C. (2019). Characterizing and minimizing the contribution of sensory inputs to TMS-evoked potentials. *Brain Stimulation*, *12*(6), 1537–1552. https://doi.org/10.1016/j.brs.2019.07.009

Bianco, V., Arrigoni, E., Di Russo, F., Romero Lauro, L. J., & Pisoni, A. (2023). Top-down reconfiguration of SMA cortical connectivity during action preparation. *IScience*, *26*(8). https://doi.org/10.1016/j.isci.2023.107430

Bonato, C., Miniussi, C., & Rossini, P. M. (2006). Transcranial magnetic stimulation and cortical evoked potentials: A TMS/EEG co-registration study. *Clinical Neurophysiology*, *117*(8), 1699–1707. https://doi.org/10.1016/j.clinph.2006.05.006

Brinkman, L., Stolk, A., Dijkerman, H. C., De Lange, F. P., & Toni, I. (2014). Distinct roles for alpha- and beta-band oscillations during mental simulation of goal-directed actions. *Journal of Neuroscience*, *34*(44), 14783–14792. https://doi.org/10.1523/JNEUROSCI.2039-14.2014

Brinkman, L., Stolk, A., Marshall, T. R., Esterer, S., Sharp, P., Dijkerman, H. C., de Lange, F. P., & Toni, I. (2016). Independent causal contributions of Alpha- and Beta-band oscillations during movement selection. *Journal of Neuroscience*, *36*(33), 8726–8733. https://doi.org/10.1523/JNEUROSCI.0868-16.2016

Cao, Z., Xiao, X., Xie, C., Wei, L., Yang, Y., & Zhu, C. (2024). Personalized connectivity-based network targeting model of transcranial magnetic stimulation for treatment of psychiatric disorders: computational feasibility and reproducibility. *Frontiers in Psychiatry*, *15*. https://doi.org/10.3389/fpsyt.2024.1341908

Casarotto, A., Dolfini, E., Fadiga, L., Koch, G., & D'Ausilio, A. (2023). Cortico-cortical paired associative stimulation conditioning superficial ventral premotor cortex-primary motor cortex connectivity influences motor cortical activity during precision grip. *The Journal of Physiology*, *601*, 3945–3960. https://doi.org/10.1113/JP284500#support-information-section

Casarotto, S., Lauro, L. J. R., Bellina, V., Casali, A. G., Rosanova, M., Pigorini, A., Defendi, S., Mariotti, M., & Massimini, M. (2010). EEG responses to TMS are sensitive to changes in the perturbation parameters and repeatable over time. *PLoS ONE*, *5*(4). https://doi.org/10.1371/journal.pone.0010281

Cash, R. F. H., Weigand, A., Zalesky, A., Siddiqi, S. H., Downar, J., Fitzgerald, P. B., & Fox, M. D. (2021). Using Brain Imaging to Improve Spatial Targeting of Transcranial Magnetic Stimulation for Depression. *Biological Psychiatry*, *90*(10), 689–700. https://doi.org/10.1016/j.biopsych.2020.05.033

Casula, E. P., Leodori, G., Ibáñez, J., Benussi, A., Rawji, V., Tremblay, S., Latorre, A., Rothwell, J. C., & Rocchi, L. (2022). The Effect of Coil Orientation on the Stimulation of the Pre–Supplementary Motor Area: A Combined TMS and EEG Study. *Brain Sciences*, *12*(10). https://doi.org/10.3390/brainsci12101358

Casula, E. P., Rocchi, L., Hannah, R., & Rothwell, J. C. (2018). Effects of pulse width, waveform and current direction in the cortex: A combined cTMS-EEG study. *Brain Stimulation*, *11*(5), 1063–1070. https://doi.org/10.1016/j.brs.2018.04.015

Chapeton, J. I., Haque, R., Wittig, J. H., Inati, S. K., & Zaghloul, K. A. (2019). Large-Scale Communication in the Human Brain Is Rhythmically Modulated through Alpha Coherence. *Current Biology*, *29*(17), 2801-2811.e5. https://doi.org/10.1016/j.cub.2019.07.014

Chen, C. C., Henson, R. N., Stephan, K. E., Kilner, J. M., & Friston, K. J. (2009). Forward and backward connections in the brain: A DCM study of functional asymmetries. *NeuroImage*, *45*(2), 453–462. https://doi.org/10.1016/j.neuroimage.2008.12.041

Chen, C. C., Kiebel, S. J., Kilner, J. M., Ward, N. S., Stephan, K. E., Wang, W. J., & Friston, K. J. (2012). A dynamic causal model for evoked and induced responses. *NeuroImage*, *59*(1), 340–348. https://doi.org/10.1016/j.neuroimage.2011.07.066

Corp, D. T., Bereznicki, H. G. K., Clark, G. M., Youssef, G. J., Fried, P. J., Jannati, A., Davies, C. B., Gomes-Osman, J., Kirkovski, M., Albein-Urios, N., Fitzgerald, P. B., Koch, G., Di Lazzaro, V., Pascual-Leone, A., & Enticott, P. G. (2021). Large-scale analysis of interindividual variability in single and paired-pulse TMS data. *Clinical Neurophysiology*, *132*(10), 2639–2653. https://doi.org/10.1016/j.clinph.2021.06.014

Corthout, E., Barker, A. T., & Cowey, A. (2001). Transcranial magnetic stimulation: Which part of the current waveform causes the stimulation? *Experimental Brain Research*, *141*(1), 128–132. https://doi.org/10.1007/s002210100860

De Martino, E., Casali, A. G., Nascimento Couto, B. A., Graven-Nielsen, T., & Ciampi de Andrade, D. (2025). Increase in beta frequency phase synchronization and power after a session of high frequency repetitive transcranial magnetic stimulation to the primary motor cortex. *Neurotherapeutics*, *22*(1). https://doi.org/10.1016/j.neurot.2024.e00497

Delorme, A., & Makeig, S. (2004). EEGLAB: an open source toolbox for analysis of single-trial EEG dynamics including independent component analysis. *Journal of Neuroscience Methods*, *134*(1), 9–21. https://doi.org/10.1016/J.JNEUMETH.2003.10.009

Di Lazzaro, V., Dileone, M., Pilato, F., Capone, F., Musumeci, G., Ranieri, F., Ricci, V., Bria, P., Di Iorio, R., de Waure, C., Pasqualetti, P., & Profice, P. (2011). Modulation of motor cortex neuronal networks by rTMS: comparison of local and remote effects of six different protocols of stimulation. *Journal of Neurophysiology*, *105*(5), 2150–2156. https://doi.org/10.1152/jn.00781.2010

Di Lazzaro, V., Rothwell, J., & Capogna, M. (2018). Noninvasive Stimulation of the Human Brain: Activation of Multiple Cortical Circuits. *Neuroscientist*, *24*(3), 246–260. https://doi.org/10.1177/1073858417717660

Eaton, S. A., & Salt, T. E. (1996). Role of N-methyl-d-aspartate and metabotropic glutamate receptors in corticothalamic excitatory postsynaptic potentials In vivo. *Neuroscience*, *73*(1), 1–5. https://doi.org/10.1016/0306-4522(96)00123-6

Farzan, F., & Bortoletto, M. (2022). Identification and verification of a “true” TMS evoked potential in TMS-EEG. *Journal of Neuroscience Methods*, *378*(October 2021), 109651. https://doi.org/10.1016/j.jneumeth.2022.109651

Federici, A., Bennett, C. R., Bauer, C. M., Manley, C. E., Ricciardi, E., Bottari, D., & Merabet, L. B. (2023). Altered neural oscillations underlying visuospatial processing in cerebral visual impairment. *Brain Communications*, *5*(5). https://doi.org/10.1093/braincomms/fcad232

Fitzsimmons, S. M. D. D., Oostra, E., Postma, T. S., van der Werf, Y. D., & van den Heuvel, O. A. (2024). Repetitive Transcranial Magnetic Stimulation–Induced Neuroplasticity and the Treatment of Psychiatric Disorders: State of the Evidence and Future Opportunities. *Biological Psychiatry*, *95*(6), 592–600. https://doi.org/10.1016/j.biopsych.2023.11.016

Fox, M. D., Halko, M. A., Eldaief, M. C., & Pascual-Leone, A. (2012). Measuring and manipulating brain connectivity with resting state functional connectivity magnetic resonance imaging (fcMRI) and transcranial magnetic stimulation (TMS). *NeuroImage*, *62*(4), 2232–2243. https://doi.org/10.1016/j.neuroimage.2012.03.035

Fries, P. (2005). A mechanism for cognitive dynamics: Neuronal communication through neuronal coherence. *Trends in Cognitive Sciences*, *9*(10), 474–480. https://doi.org/10.1016/j.tics.2005.08.011

Fries, P. (2015). Rhythms for Cognition: Communication through Coherence. *Neuron*, *88*(1), 220–235. https://doi.org/10.1016/j.neuron.2015.09.034

Friston, K. J. (2011). Functional and Effective Connectivity: A Review. *Brain Connectivity*, *1*(1), 13–36. https://doi.org/10.1089/brain.2011.0008

Groppe, D. M., Bickel, S., Keller, C. J., Jain, S. K., Hwang, S. T., Harden, C., & Mehta, A. D. (2013). Dominant frequencies of resting human brain activity as measured by the electrocorticogram. *NeuroImage*, *79*, 223–233. https://doi.org/10.1016/J.NEUROIMAGE.2013.04.044

Gross, J., Baillet, S., Barnes, G. R., Henson, R. N., Hillebrand, A., Jensen, O., Jerbi, K., Litvak, V., Maess, B., Oostenveld, R., Parkkonen, L., Taylor, J. R., van Wassenhove, V., Wibral, M., & Schoffelen, J. M. (2013). Good practice for conducting and reporting MEG research. In *NeuroImage* (Vol. 65, pp. 349–363). https://doi.org/10.1016/j.neuroimage.2012.10.001

Guidali, G., Arrigoni, E., Bolognini, N., & Pisoni, A. (2025). M1 large-scale network dynamics support human motor resonance and its plastic reshaping. *NeuroImage*, *308*, 121082. https://doi.org/10.1016/j.neuroimage.2025.121082

Guidali, G., Zazio, A., Lucarelli, D., Marcantoni, E., Stango, A., Barchiesi, G., & Bortoletto, M. (2023). Effects of transcranial magnetic stimulation (TMS) current direction and pulse waveform on cortico-cortical connectivity: A registered report TMS-EEG study. *European Journal of Neuroscience*, *58*(8), 3785–3809. https://doi.org/10.1111/ejn.16127

Haegens, S., Nácher, V., Hernández, A., Luna, R., Jensen, O., & Romo, R. (2011). Beta oscillations in the monkey sensorimotor network reflect somatosensory decision making. *Proceedings of the National Academy of Sciences*, *108*(26), 10708–10713. https://doi.org/10.1073/pnas.1107297108

Haegens, S., Nácher, V., Luna, R., Romo, R., & Jensen, O. (2011). α-Oscillations in the monkey sensorimotor network influence discrimination performance by rhythmical inhibition of neuronal spiking. *Proceedings of the National Academy of Sciences*, *108*(48), 19377–19382. https://doi.org/10.1073/pnas.1117190108

Halawa, I., Shirota, Y., Neef, A., Sommer, M., & Paulus, W. (2019). Neuronal tuning: Selective targeting of neuronal populations via manipulation of pulse width and directionality. *Brain Stimulation*, *12*(5), 1244–1252. https://doi.org/10.1016/J.BRS.2019.04.012

Hamada, M., Strigaro, G., Murase, N., Sadnicka, A., Galea, J. M., Edwards, M. J., & Rothwell, J. C. (2012). Cerebellar modulation of human associative plasticity. *Journal of Physiology*, *590*(10), 2365–2374. https://doi.org/10.1113/jphysiol.2012.230540

Harris, K. D., & Shepherd, G. M. G. (2015). The neocortical circuit: Themes and variations. *Nature Neuroscience*, *18*(2), 170–181. https://doi.org/10.1038/nn.3917

Hernandez-Pavon, J. C., Veniero, D., Bergmann, T. O., Belardinelli, P., Bortoletto, M., Casarotto, S., Casula, E. P., Farzan, F., Fecchio, M., Julkunen, P., Kallioniemi, E., Lioumis, P., Metsomaa, J., Miniussi, C., Mutanen, T. P., Rocchi, L., Rogasch, N. C., Shafi, M. M., Siebner, H. R., … Ilmoniemi, R. J. (2023). TMS combined with EEG: Recommendations and open issues for data collection and analysis. *Brain Stimulation*, *16*(2), 567–593. https://doi.org/10.1016/J.BRS.2023.02.009

Humaidan, D., Xu, J., Kirchhoff, M., Romani, G. L., Ilmoniemi, R. J., & Ziemann, U. (2024). Towards real-time EEG–TMS modulation of brain state in a closed-loop approach. In *Clinical Neurophysiology* (Vol. 158, pp. 212–217). Elsevier Ireland Ltd. https://doi.org/10.1016/j.clinph.2023.12.006

Hunt, D. L., & Castillo, P. E. (2012). Synaptic plasticity of NMDA receptors: mechanisms and functional implications. *Current Opinion in Neurobiology*, *22*(3), 496–508. https://doi.org/10.1016/j.conb.2012.01.007

Hyvärinen, A., & Oja, E. (2000). Independent component analysis: algorithms and applications. *Neural Networks*, *13*(4–5), 411–430. https://doi.org/10.1016/S0893-6080(00)00026-5

Jensen, O., Goel, P., Kopell, N., Pohja, M., Hari, R., & Ermentrout, B. (2005). On the human sensorimotor-cortex beta rhythm: Sources and modeling. *NeuroImage*, *26*(2), 347–355. https://doi.org/10.1016/j.neuroimage.2005.02.008

Kanig, C., Osnabruegge, M., Schwitzgebel, F., Mack, W., Schecklmann, M., & Schoisswohl, S. (2025). Influences of current direction on 1 Hz motor cortex rTMS. *Brain Research Bulletin*, *230*. https://doi.org/10.1016/j.brainresbull.2025.111484

Kilavik, B. E., Zaepffel, M., Brovelli, A., MacKay, W. A., & Riehle, A. (2013). The ups and downs of beta oscillations in sensorimotor cortex. *Experimental Neurology*, *245*, 15–26. https://doi.org/10.1016/j.expneurol.2012.09.014

Koch, G., Ponzo, V., Di Lorenzo, F., Caltagirone, C., & Veniero, D. (2013). Hebbian and Anti-Hebbian Spike-Timing-Dependent Plasticity of Human Cortico-Cortical Connections. *Journal of Neuroscience*, *33*(23), 9725–9733. https://doi.org/10.1523/JNEUROSCI.4988-12.2013

Koponen, L. M., Nieminen, J. O., & Ilmoniemi, R. J. (2018). Multi-locus transcranial magnetic stimulation—theory and implementation. *Brain Stimulation*, *11*(4), 849–855. https://doi.org/10.1016/j.brs.2018.03.014

Li, S., Lan, X., Liu, Y., Zhou, J., Pei, Z., Su, X., & Guo, Y. (2024). Unlocking the Potential of Repetitive Transcranial Magnetic Stimulation in Alzheimer's Disease: A Meta-Analysis of Randomized Clinical Trials to Optimize Intervention Strategies. *Journal of Alzheimer's Disease*, *98*(2), 481–503. https://doi.org/10.3233/JAD-231031

Lu, C. M., Zhang, Y. J., Biswal, B. B., Zang, Y. F., Peng, D. L., & Zhu, C. Z. (2010). Use of fNIRS to assess resting state functional connectivity. *Journal of Neuroscience Methods*, *186*(2), 242–249. https://doi.org/10.1016/j.jneumeth.2009.11.010

Lucarelli, D., Guidali, G., Sulcova, D., Zazio, A., Bonfiglio, N. S., Stango, A., Barchiesi, G., & Bortoletto, M. (2025). Stimulation Parameters Recruit Distinct Cortico-Cortical Pathways: Insights from Microstate Analysis on TMS-Evoked Potentials. *Brain Topography*, *38*(3), 39. https://doi.org/10.1007/s10548-025-01113-2

Luo, X., Che, X., & Li, H. (2023). Concurrent TMS-EEG and EEG reveal neuroplastic and oscillatory changes associated with self-compassion and negative emotions. *International Journal of Clinical and Health Psychology*, *23*(1). https://doi.org/10.1016/j.ijchp.2022.100343

Marzetti, L., Basti, A., Chella, F., D'Andrea, A., Syrjälä, J., & Pizzella, V. (2019). Brain Functional Connectivity Through Phase Coupling of Neuronal Oscillations: A Perspective From Magnetoencephalography. *Frontiers in Neuroscience*, *13*. https://doi.org/10.3389/fnins.2019.00964

Marzetti, L., Makkinayeri, S., Pieramico, G., Guidotti, R., D'Andrea, A., Roine, T., Mutanen, T. P., Souza, V. H., Kičić, D., Baldassarre, A., Ermolova, M., Pankka, H., Ilmoniemi, R. J., Ziemann, U., Luca Romani, G., & Pizzella, V. (2024). Towards real-time identification of large-scale brain states for improved brain state-dependent stimulation. *Clinical Neurophysiology*, *158*, 196–203. https://doi.org/10.1016/j.clinph.2023.09.005

Menon, P., Pavey, N., Aberra, A. S., van den Bos, M. A. J., Wang, R., Kiernan, M. C., Peterchev, A. V., & Vucic, S. (2023). Dependence of cortical neuronal strength-duration properties on TMS pulse shape. *Clinical Neurophysiology*, *150*, 106–118. https://doi.org/10.1016/j.clinph.2023.03.012

Momi, D., Ozdemir, R. A., Tadayon, E., Boucher, P., Shafi, M. M., Pascual-Leone, A., & Santarnecchi, E. (2021). Network-level macroscale structural connectivity predicts propagation of transcranial magnetic stimulation. *NeuroImage*, *229*(July 2020), 117698. https://doi.org/10.1016/j.neuroimage.2020.117698

Momi, D., Wang, Z., & Griffiths, J. D. (2023). TMS-evoked responses are driven by recurrent large-scale network dynamics. *ELife*, *12*, 1–33. https://doi.org/10.7554/eLife.83232

Mutanen, T. P., Kukkonen, M., Nieminen, J. O., Stenroos, M., Sarvas, J., & Ilmoniemi, R. J. (2016). Recovering TMS-evoked EEG responses masked by muscle artifacts. *NeuroImage*, *139*, 157–166. https://doi.org/10.1016/j.neuroimage.2016.05.028

Mutanen, T. P., Metsomaa, J., Liljander, S., & Ilmoniemi, R. J. (2018). Automatic and robust noise suppression in EEG and MEG: The SOUND algorithm. *NeuroImage*, *166*(October 2017), 135–151. https://doi.org/10.1016/j.neuroimage.2017.10.021

Nieminen, J. O., Sinisalo, H., Souza, V. H., Malmi, M., Yuryev, M., Tervo, A. E., Stenroos, M., Milardovich, D., Korhonen, J. T., Koponen, L. M., & Ilmoniemi, R. J. (2022). Multi-locus transcranial magnetic stimulation system for electronically targeted brain stimulation. *Brain Stimulation*, *15*(1), 116–124. https://doi.org/10.1016/j.brs.2021.11.014

Oldfield, R. C. (1971). The assessment and analysis of handedness: The Edinburgh inventory. *Neuropsychologia*, *9*(1), 97–113. https://doi.org/10.1016/0028-3932(71)90067-4

Oostenveld, R., Fries, P., Maris, E., & Schoffelen, J. M. (2011). FieldTrip: Open source software for advanced analysis of MEG, EEG, and invasive electrophysiological data. *Computational Intelligence and Neuroscience*, *2011*. https://doi.org/10.1155/2011/156869

Palva, S., & Palva, J. M. (2011). Functional Roles of Alpha-Band Phase Synchronization in Local and Large-Scale Cortical Networks. *Frontiers in Psychology*, *2*(9). https://doi.org/10.3389/fpsyg.2011.00204

Pascual-Marqui, R. D. (2002). Standardized low-resolution brain electromagnetic tomography (sLORETA): technical details. *Methods and Findings in Experimental and Clinical Pharmacology*, *24 Suppl D*, 5–12. http://www.ncbi.nlm.nih.gov/pubmed/12575463

Pellicciari, M. C., Veniero, D., & Miniussi, C. (2017). Characterizing the Cortical Oscillatory Response to TMS Pulse. *Frontiers in Cellular Neuroscience*, *11*(February), 1–5. https://doi.org/10.3389/fncel.2017.00038

Pieramico, G., Guidotti, R., Nieminen, A. E., D'Andrea, A., Basti, A., Souza, V. H., Nieminen, J. O., Lioumis, P., Ilmoniemi, R. J., Romani, G. L., Pizzella, V., & Marzetti, L. (2023). TMS-Induced Modulation of EEG Functional Connectivity Is Affected by the E-Field Orientation. *Brain Sciences*, *13*(3). https://doi.org/10.3390/brainsci13030418

Pisoni, A., Romero Lauro, L., Vergallito, A., Maddaluno, O., & Bolognini, N. (2018). Cortical dynamics underpinning the self-other distinction of touch : A TMS-EEG study. *Neuroimage*, *178*(3), 475–484. https://doi.org/10.1016/j.neuroimage.2018.05.078

Reithler, J., Peters, J. C., & Sack, A. T. (2011). Multimodal transcranial magnetic stimulation: Using concurrent neuroimaging to reveal the neural network dynamics of noninvasive brain stimulation. *Progress in Neurobiology*, *94*(2), 149–165. https://doi.org/10.1016/j.pneurobio.2011.04.004

Rossi, S., Antal, A., Bestmann, S., Bikson, M., Brewer, C., Brockmöller, J., Carpenter, L. L., Cincotta, M., Chen, R., Daskalakis, J. D., Di Lazzaro, V., Fox, M. D., George, M. S., Gilbert, D., Kimiskidis, V. K., Koch, G., Ilmoniemi, R. J., Lefaucheur, J. P., Leocani, L., … Hallett, M. (2021). Safety and recommendations for TMS use in healthy subjects and patient populations, with updates on training, ethical and regulatory issues: Expert Guidelines. *Clinical Neurophysiology*, *132*(1), 269–306. https://doi.org/10.1016/j.clinph.2020.10.003

Salmelin, R., & Hari, R. (1994). Characterization of spontaneous MEG rhythms in healthy adults. *Electroencephalography and Clinical Neurophysiology*, *91*(4), 237–248. https://doi.org/10.1016/0013-4694(94)90187-2

Schiena, G., Franco, G., Boscutti, A., Delvecchio, G., Maggioni, E., & Brambilla, P. (2021). Connectivity changes in major depressive disorder after rTMS: a review of functional and structural connectivity data. *Epidemiology and Psychiatric Sciences*, *30*. https://doi.org/10.1017/S2045796021000482

Schoffelen, J. M., & Gross, J. (2009). Source connectivity analysis with MEG and EEG. In *Human Brain Mapping* (Vol. 30, Issue 6, pp. 1857–1865). https://doi.org/10.1002/hbm.20745

Schulz, H., Übelacker, T., Keil, J., Müller, N., & Weisz, N. (2014). Now i am ready - Now i am not: The influence of pre-TMS oscillations and corticomuscular coherence on motor-evoked potentials. *Cerebral Cortex*, *24*(7), 1708–1719. https://doi.org/10.1093/cercor/bht024

Shirota, Y., Dhaka, S., Paulus, W., & Sommer, M. (2017). Current direction-dependent modulation of human hand motor function by intermittent theta burst stimulation (iTBS). *Neuroscience Letters*, *650*, 109–113. https://doi.org/10.1016/J.NEULET.2017.04.032

Siddiqi, S. H., Kording, K. P., Parvizi, J., & Fox, M. D. (2022). Causal mapping of human brain function. In *Nature Reviews Neuroscience* (Vol. 23, Issue 6, pp. 361–375). Nature Research. https://doi.org/10.1038/s41583-022-00583-8

Siebner, H. R., Funke, K., Aberra, A. S., Antal, A., Bestmann, S., Chen, R., Classen, J., Davare, M., Di Lazzaro, V., Fox, P. T., Hallett, M., Karabanov, A. N., Kesselheim, J., Beck, M. M., Koch, G., Liebetanz, D., Meunier, S., Miniussi, C., Paulus, W., … Ugawa, Y. (2022). Transcranial magnetic stimulation of the brain: What is stimulated? – A consensus and critical position paper. *Clinical Neurophysiology*, *140*, 59–97. https://doi.org/10.1016/j.clinph.2022.04.022

Siegel, M., Donner, T. H., & Engel, A. K. (2012). Spectral fingerprints of large-scale neuronal interactions. *Nature Reviews Neuroscience*, *13*(2), 121–134. https://doi.org/10.1038/nrn3137

Sinisalo, H., Rissanen, I., Kahilakoski, O.-P., Souza, V. H., Tommila, T., Laine, M., Nyrhinen, M., Ukharova, E., Granö, I., Soto, A. M., Matsuda, R. H., Rantala, R., Guidotti, R., Kičić, D., Lioumis, P., Mutanen, T., Pizzella, V., Marzetti, L., Roine, T., … Ilmoniemi, R. J. (2024). Modulating brain networks in space and time: Multi-locus transcranial magnetic stimulation. *Clinical Neurophysiology*, *158*, 218–224. https://doi.org/10.1016/j.clinph.2023.12.007

Sommer, M., Alfaro, A., Rummel, M., Speck, S., Lang, N., Tings, T., & Paulus, W. (2006). Half sine, monophasic and biphasic transcranial magnetic stimulation of the human motor cortex. *Clinical Neurophysiology*, *117*(4), 838–844. https://doi.org/10.1016/j.clinph.2005.10.029

Sommer, M., Ciocca, M., Chieffo, R., Hammond, P., Neef, A., Paulus, W., Rothwell, J. C., & Hannah, R. (2018). TMS of primary motor cortex with a biphasic pulse activates two independent sets of excitable neurones. *Brain Stimulation*, *11*(3), 558–565. https://doi.org/10.1016/j.brs.2018.01.001

Sommer, M., Hannah, R., Peterchev, A., & Paulus, W. (2023). TMS pulse waveform and direction. In *The Oxford Handbook of Transcranial Stimulation*. Oxford University Press.

Sommer, M., Norden, C., Schmack, L., Rothkegel, H., Lang, N., & Paulus, W. (2013). Opposite optimal current flow directions for induction of neuroplasticity and excitation threshold in the human motor cortex. *Brain Stimulation*, *6*(3), 363–370. https://doi.org/10.1016/j.brs.2012.07.003

Souza, V. H., Nieminen, J. O., Tugin, S., Koponen, L. M., Ziemann, U., Baffa, O., & Ilmoniemi, R. J. (2025). Probing the orientation specificity of excitatory and inhibitory circuitries in the primary motor cortex with multi-channel TMS. *Clinical Neurophysiology*, *169*, 23–32. https://doi.org/10.1016/j.clinph.2024.11.004

Souza, V. H., Vieira, T. M., Peres, A. S. C., Garcia, M. A. C., Vargas, C. D., & Baffa, O. (2018). Effect of TMS coil orientation on the spatial distribution of motor evoked potentials in an intrinsic hand muscle. *Biomedizinische Technik*, *63*(6), 635–645. https://doi.org/10.1515/bmt-2016-0240

Spampinato, D. (2020). Dissecting two distinct interneuronal networks in M1 with transcranial magnetic stimulation. *Experimental Brain Research*, *238*(7–8), 1693–1700. https://doi.org/10.1007/s00221-020-05875-y

Sporns, O., Tononi, G., & Edelman, G. M. (2000). Connectivity and complexity: the relationship between neuroanatomy and brain dynamics. *Neural Networks*, *13*(8–9), 909–922. https://doi.org/10.1016/S0893-6080(00)00053-8

Stolk, A., Brinkman, L., Vansteensel, M. J., Aarnoutse, E., Leijten, F. S. S., Dijkerman, C. H., Knight, R. T., de Lange, F. P., & Toni, I. (2019). Electrocorticographic dissociation of alpha and beta rhythmic activity in the human sensorimotor system. *ELife*, *8*. https://doi.org/10.7554/ELIFE.48065

Suppa, A., Ortu, E., Zafar, N., Deriu, F., Paulus, W., Berardelli, A., & Rothwell, J. C. (2008). Theta burst stimulation induces after-effects on contralateral primary motor cortex excitability in humans. *Journal of Physiology*, *586*(18), 4489–4500. https://doi.org/10.1113/jphysiol.2008.156596

Talelli, P., Cheeran, B. J., Teo, J. T. H., & Rothwell, J. C. (2007). Pattern-specific role of the current orientation used to deliver Theta Burst Stimulation. *Clinical Neurophysiology*, *118*(8), 1815–1823. https://doi.org/10.1016/J.CLINPH.2007.05.062

Tallon-Baudry, C. (1999). Oscillatory gamma activity in humans and its role in object representation. *Trends in Cognitive Sciences*, *3*(4), 151–162. https://doi.org/10.1016/S1364-6613(99)01299-1

The Jamovi Project. (2025). *Jamovi (version 2.7) [Computer Software]. Retrieved from https://www.jamovi.org*.

Trajkovic, J., Veniero, D., Hanslmayr, S., Palva, S., Cruz, G., Romei, V., & Thut, G. (2025). Top-down and bottom-up interactions rely on nested brain oscillations to shape rhythmic visual attention sampling. *PLoS Biology*, *23*(4). https://doi.org/10.1371/journal.pbio.3002688

Tzourio-Mazoyer, N., Landeau, B., Papathanassiou, D., Crivello, F., Etard, O., Delcroix, N., Mazoyer, B., & Joliot, M. (2002). Automated anatomical labeling of activations in SPM using a macroscopic anatomical parcellation of the MNI MRI single-subject brain. *NeuroImage*, *15*(1), 273–289. https://doi.org/10.1006/nimg.2001.0978

van den Heuvel, M. P., & Hulshoff Pol, H. E. (2010). Exploring the brain network: A review on resting-state fMRI functional connectivity. In *European Neuropsychopharmacology* (Vol. 20, Issue 8, pp. 519–534). https://doi.org/10.1016/j.euroneuro.2010.03.008

van Wijk, B. C. M., Beek, P. J., & Daffertshofer, A. (2012). Neural synchrony within the motor system: what have we learned so far? *Frontiers in Human Neuroscience*, *6*(9). https://doi.org/10.3389/fnhum.2012.00252

Varela, F., Lachaux, J.-P., Rodriguez, E., & Martinerie, J. (2001). The brainweb: Phase synchronization and large-scale integration. *Nature Reviews Neuroscience*, *2*(4), 229–239. https://doi.org/10.1038/35067550

Veniero, D., Vossen, A., Gross, J., & Thut, G. (2015). Lasting EEG/MEG Aftereffects of Rhythmic Transcranial Brain Stimulation: Level of Control Over Oscillatory Network Activity. *Frontiers in Cellular Neuroscience*, *9*(DEC), 1–17. https://doi.org/10.3389/fncel.2015.00477

Vetter, D. E., Zrenner, C., Belardinelli, P., Mutanen, T. P., Kozák, G., Marzetti, L., & Ziemann, U. (2023). Targeting motor cortex high-excitability states defined by functional connectivity with real-time EEG–TMS. *NeuroImage*, *284*. https://doi.org/10.1016/j.neuroimage.2023.120427

Vidaurre, D., Hunt, L. T., Quinn, A. J., Hunt, B. A. E., Brookes, M. J., Nobre, A. C., & Woolrich, M. W. (2018). Spontaneous cortical activity transiently organises into frequency specific phase-coupling networks. *Nature Communications*, *9*(1). https://doi.org/10.1038/s41467-018-05316-z

Vinck, M., Oostenveld, R., van Wingerden, M., Battaglia, F., & Pennartz, C. M. A. (2011). An improved index of phase-synchronization for electrophysiological data in the presence of volume-conduction, noise and sample-size bias. *NeuroImage*, *55*(4), 1548–1565. https://doi.org/https://doi.org/10.1016/j.neuroimage.2011.01.055

Weiler, N., Wood, L., Yu, J., Solla, S. A., & Shepherd, G. M. G. (2008). Top-down laminar organization of the excitatory network in motor cortex. *Nature Neuroscience*, *11*(3), 360–366. https://doi.org/10.1038/nn2049

Wischnewski, M., Haigh, Z. J., Shirinpour, S., Alekseichuk, I., & Opitz, A. (2022). The phase of sensorimotor mu and beta oscillations has the opposite effect on corticospinal excitability. *Brain Stimulation*, *15*(5), 1093–1100. https://doi.org/10.1016/j.brs.2022.08.005

Ye, L., Zhao, W., Zhang, Y., Song, W., Xie, H., & Cao, L. (2025). Exploring Neurobiological Effects of Intermittent Theta-Burst Stimulation on the Left Cerebellum for Post-stroke Unilateral Neglect: A Preliminary Transcranial Magnetic Stimulation—Electroencephalography Investigation. *Cerebellum*, *24*(4). https://doi.org/10.1007/s12311-025-01853-8

Ye, Y., Wang, J., & Che, X. (2022). Concurrent TMS-EEG to reveal the neuroplastic changes in the prefrontal and insular cortices in the analgesic effects of DLPFC-rTMS. *Cerebral Cortex*, *32*(20), 4436–4446. https://doi.org/10.1093/cercor/bhab493

Yusuf, P. A., Hubka, P., Tillein, J., & Kral, A. (2017). Induced cortical responses require developmental sensory experience. *Brain*, *140*(12), 3153–3165. https://doi.org/10.1093/brain/awx286

Ziemann, U., Bai, Y., Baumer, F. M., Beck, M. M., Belardinelli, P., Belvisi, D., Bender, S., Bergmann, T. O., Bortoletto, M., Casarotto, S., Casula, E., Chaves, A. R., de Andrade, D. C., Conte, A., Daskalakis, Z. J., Farzan, F., Ferrarelli, F., Fitzgerald, P. B., Gordon, P. C., … Ilmoniemi, R. J. (2026). Clinical utility and prospective of TMS–EEG: Updated review from an international expert group. *Clinical Neurophysiology*, 2111487. https://doi.org/10.1016/j.clinph.2025.2111487

Zrenner, C., Desideri, D., Belardinelli, P., & Ziemann, U. (2018). Real-time EEG-defined excitability states determine efficacy of TMS-induced plasticity in human motor cortex. *Brain Stimulation*, *11*(2), 374–389. https://doi.org/10.1016/j.brs.2017.11.016



**Table 1.** List of parcels whose alpha-band functional connectivity (i.e., dwPLI) with lpM1 was significantly modulated after TMS (compared to 'pre-TMS' period) in monophasic conditions. Paired sample t-test statistics are reported for each parcel.

| ALPHA BAND | MONOPHASIC PA | | | | | MONOPHASIC AP | | | | |
|---|---|---|---|---|---|---|---|---|---|---|
| | ***parcel*** | ***hemisphere*** | $t_{31}$ | ***p*** | ***d*** | ***parcel*** | ***hemisphere*** | $t_{31}$ | ***p*** | ***d*** |
| **Frontal lobe** | Precentral gyrus | R | 2.734 | .01 | .191 | Precentral gyrus | R | 2.653 | .012 | .253 |
| | Superior frontal gyrus, orbital | L | 4.223 | <.001 | .223 | Superior frontal gyrus | R | 2.641 | .013 | .244 |
| | Middle frontal gyrus, orbital | L | 4.102 | <.001 | .254 | Middle frontal gyrus | R | 3.014 | .005 | .326 |
| | Inferior frontal gyrus, orbital | L | 2.742 | .01 | .232 | Inferior frontal gyrus, opercular part | R | 3.402 | .002 | .299 |
| | Supplementary Motor Area | L | 2.654 | .012 | .255 | Inferior frontal gyrus, triangular part | R | 2.473 | .019 | .227 |
| | | R | 2.853 | .008 | .235 | Rolandic operculum | R | 2.408 | .022 | .161 |
| | Olfactory cortex | L | 2.387 | .023 | .196 | Olfactory cortex | R | 2.057 | .048 | .185 |
| | | L | 2.485 | .019 | .164 | | L | 3.413 | .002 | .291 |

| | | | | | | | | | | |
|---|---|---|---|---|---|---|---|---|---|---|
| | Superior frontal gyrus, medial orbital | R | 2.054 | .048 | .168 | Superior frontal gyrus, medial | R | 2.671 | .012 | .227 |
| | Rectus | L | 3.212 | .003 | .249 | Insula | R | 2.15 | .04 | .155 |
| | | R | 2.458 | .02 | .179 | Median cingulate gyrus | L | 2.3 | .028 | .208 |
| | Insula | L | 2.586 | .015 | .266 | | R | 3.458 | .002 | .305 |
| | Anterior cingulate gyrus | L | 2.273 | .03 | .213 | Posterior cingulate gyrus | L | 2.14 | .04 | .208 |
| **Temporal lobe** | Hippocampus | L | 2.187 | .036 | .164 | Heschl gyrus | R | 2.258 | .031 | .158 |
| | Parahippocampal gyrus | L | 2.442 | .021 | .202 | | | | | |
| | Heschl gyrus | R | 2.579 | .015 | .168 | | | | | |
| **Occipital lobe** | Lingual gyrus | L | 2.046 | .049 | .187 | Calcarine scissure | L | 2.628 | .013 | .178 |
| | | | | | | Cuneus | L | 3.608 | .001 | .256 |
| | | | | | | Superior occipital gyrus | L | 3.219 | .003 | .259 |
| | | | | | | Middle occipital gyrus | L | 2.052 | .049 | .192 |
| **Parietal lobe** | Postcentral gyrus | R | 2.513 | .017 | .182 | Postcentral gyrus | R | 2.585 | .015 | .232 |
| | Superior parietal gyrus | R | 2.403 | .022 | .204 | Superior parietal gyrus | L | 2.544 | .016 | .225 |
| | Inferior parietal gyrus | R | 3.082 | .004 | .252 | Inferior parietal gyrus | L | 2.452 | .02 | .232 |
| | Supramarginal gyrus | R | 3.258 | .003 | .221 | | R | 2.246 | .032 | .175 |
| | Angular gyrus | R | 2.188 | .036 | .14 | Supramarginal gyrus | R | 2.201 | .035 | .172 |
| | Precuneus | L | 2.158 | .039 | .193 | Precuneus | L | 2.979 | .006 | .273 |
| | Paracentral lobule | R | 2.73 | .01 | .248 | | | | | |
| | Caudate | L | 2.254 | .031 | .183 | Caudate | L | 2.067 | .047 | .178 |

| | | | | | | | | | | |
|---|---|---|---|---|---|---|---|---|---|---|
| **Subcortical structures** | Putamen | L | 2.134 | .041 | .2 | | R | 2.775 | .009 | .219 |
| | | | | | | Putamen | R | 2.462 | .02 | .182 |
| | | | | | | Pallidum | R | 2.205 | .035 | .18 |

| ALPHA BAND | BIPHASIC PA | | | | | BIPHASIC AP | | | | |
|---|---|---|---|---|---|---|---|---|---|---|
| | ***parcel*** | ***hemisphere*** | $t_{31}$ | ***p*** | ***d*** | ***parcel*** | ***hemisphere*** | $t_{31}$ | ***p*** | ***d*** |
| **Frontal lobe** | Precentral gyrus | R | 2.969 | .006 | .243 | Precentral gyrus | R | 3.235 | .003 | .28 |
| | Superior frontal gyrus | R | 2.611 | .014 | .246 | Inferior frontal gyrus, triangular part | R | 2.274 | .03 | .194 |
| | Inferior frontal gyrus, opercular part | R | 2.086 | .045 | .195 | Supplementary Motor Area | R | 2.649 | .013 | .286 |
| | Rolandic operculum | R | 2.322 | .027 | .209 | Median cingulate gyrus | R | 2.394 | .023 | .235 |
| | Posterior cingulate gyrus | R | 2.215 | .034 | .185 | | | | | |
| **Temporal lobe** | | | | | | Hippocampus | L | 2.437 | .021 | .213 |
| | | | | | | Parahippocampal gyrus | L | 3.084 | .004 | .24 |
| | | | | | | | R | -2.388 | .023 | .151 |
| **Occipital lobe** | Cuneus | R | 2.18 | .037 | .176 | Calcarine scissure | L | 2.367 | .024 | .189 |
| | | | | | | Cuneus | L | 2.225 | .033 | .154 |
| | | | | | | Fusiform gyrus | L | 2.71 | .011 | .222 |
| **Parietal lobe** | Postcentral gyrus | L | 2.438 | .021 | .235 | Postcentral gyrus | R | 2.352 | .025 | .194 |
| | | R | 3.155 | .004 | .314 | Superior parietal gyrus | R | 4.099 | < .001 | .29 |
| | Superior parietal gyrus | R | 2.307 | .028 | .208 | Inferior parietal gyrus | R | 2.325 | .027 | .198 |
| | Inferior parietal gyrus | R | 2.694 | .011 | .256 | Angular gyrus | R | 2.044 | .049 | .143 |
| | Supramarginal gyrus | R | 3.011 | .005 | .239 | Precuneus | R | 3.223 | .003 | .226 |
| | Angular gyrus | R | 2.552 | .016 | .193 | Paracentral lobule | R | 2.154 | .039 | .201 |
| | Paracentral lobule | R | 2.24 | .032 | .204 | | | | | |

**Table 2.** List of parcels whose alpha-band functional connectivity (i.e., dwPLI) with lpM1 was significantly modulated after TMS (compared to 'pre-TMS' period) in biphasic conditions. Paired sample t-test statistics are reported for each parcel

| BETA BAND | MONOPHASIC PA | | | | | MONOPHASIC AP | | | | |
|---|---|---|---|---|---|---|---|---|---|---|
| | ***parcel*** | ***hemisphere*** | ***$t_{31}$*** | ***p*** | ***d*** | ***parcel*** | ***hemisphere*** | ***$t_{31}$*** | ***p*** | ***d*** |
| **Frontal Lobe** | Posterior cingulate gyrus | R | 2.688 | .011 | .289 | Superior frontal gyrus, orbital | R | -2.378 | .024 | .329 |
| | | | | | | Middle frontal gyrus | L | -2.609 | .014 | .325 |
| | | | | | | Middle frontal gyrus, orbital | R | -3.061 | .005 | .374 |
| **Temporal Lobe** | Hippocampus | L | 2.192 | .036 | .304 | Middle temporal gyrus | L | 2.366 | .024 | .363 |
| | Parahippocampal gyrus | L | 2.298 | .029 | .321 | | | | | |
| **Occipital Lobe** | Lingual gyrus | L | 2.372 | .024 | .305 | Cuneus | R | 2.198 | .036 | .265 |
| | | | | | | Lingual gyrus | R | 2.781 | .009 | .38 |
| | | | | | | Superior occipital gyrus | R | 2.305 | .028 | .285 |
| | | | | | | Middle occipital gyrus | R | 3.307 | .002 | .316 |
| | | | | | | Inferior occipital gyrus | R | 2.925 | .006 | .316 |
| **Parietal Lobe** | Postcentral gyrus | R | 2.469 | .019 | .349 | Superior parietal gyrus | R | 2.742 | .01 | .321 |
| | Paracentral lobule | R | 2.278 | .03 | .286 | Angular gyrus | R | 3.854 | <.001 | .402 |
| **Subcortical Structures** | Caudate | R | 2.067 | .047 | .289 | | | | | |
| | Thalamus | R | 2.431 | .021 | .286 | | | | | |

**Table 3.** List of parcels whose beta-band functional connectivity (i.e., dwPLI) with lpM1 was significantly modulated after TMS (compared to 'pre-TMS' period) in monophasic conditions. Paired sample t-test statistics are reported for each parcel.

**Table 4.** List of parcels whose beta-band functional connectivity (i.e., dwPLI) with lpM1 was significantly modulated after TMS (compared to 'pre-TMS' period) in biphasic conditions. Paired sample t-test statistics are reported for each parcel.

| **BETA BAND** | **BIPHASIC PA** | | | | | **BIPHASIC AP** | | | | |
|---|---|---|---|---|---|---|---|---|---|---|
| | ***parcel*** | ***hemisphere*** | $t_{31}$ | ***p*** | ***d*** | ***parcel*** | ***hemisphere*** | $t_{31}$ | ***p*** | ***d*** |
| **Frontal Lobe** | Precentral | R | 2.352 | .025 | .333 | Olfactory cortex | L | -2.149 | .04 | .306 |
| | Supplemental motor area | R | 2.7 | .011 | .36 | Insula | R | -2.391 | .023 | .319 |
| | Median cingulate gyrus | R | 3.347 | .002 | .441 | | | | | |
| | Posterior cingulate gyrus | L | 3.953 | <.001 | .477 | | | | | |
| | | R | 3.69 | <.001 | .5 | | | | | |
| **Temporal Lobe** | Inferior temporal gyrus | L | -2.504 | .018 | .417 | Amygdala | R | -2.341 | .026 | .354 |
| | | R | 2.083 | .046 | .293 | | | | | |
| **Occipital Lobe** | Calcarine scissure | L | 2.478 | .019 | .324 | Cuneus | L | 2.362 | .025 | .264 |
| | Cuneus | L | 2.256 | .031 | .312 | | | | | |
| | Superior occipital gyrus | L | 2.705 | .011 | .31 | | | | | |
| | Middle occipital gyrus | L | 2.159 | .039 | .258 | | | | | |
| **Parietal Lobe** | Superior parietal gyrus | L | 2.564 | .015 | .297 | Precuneus | L | 2.082 | .046 | .318 |
| | Precuneus | L | 2.283 | .029 | .289 | | | | | |
| | | R | 2.836 | .008 | .342 | | | | | |
| **Subcortical Structures** | Thalamus | R | 2.844 | .008 | .398 | Caudate | L | -2.363 | .025 | .313 |
| | | | | | | Putamen | L | -3.051 | .005 | .433 |
| | | | | | | Pallidum | L | -2.923 | .006 | .411 |

**Data Availability Statement.**

Raw data can be found at: https://gin.g-node.org/Giacomo_Guidali/Guidali_et_al_2023_EJN_RR. Database and statistical analyses of the present study can be found on Open Science Framework – OSF (view-only link for Editors and Reviewers: https://osf.io/8z4rb/). The link will be made publicly available upon manuscript's acceptance.

## Conflict of Interests

The Authors declare that the research was conducted without any commercial or financial relationships that could be construed as a potential conflict.